Understanding mechanisms responsible for the regulation of presynaptic strengths on a dendritic tree in rat hippocampal networks

Author:

Abhilash Sawant

IISER, Pune

Supervisor:

Dr. Yukiko Goda

RIKEN BSI, Wako

TAC member:

Dr. Nixon Abraham

IISER, Pune

Certificate

This is to certify that this dissertation entitled "Understanding mechanisms responsible for the regulation of presynaptic strengths on a dendritic tree in rat hippocampal networks" towards the partial fulfilment of the BS-MS dual degree programme at the Indian Institute of Science Education and Research, Pune represents original research carried out by "Abhilash Sawant (Reg. No. – 20121098) at RIKEN Brain Science Institute, Wako, Saitama, Japan" under the supervision of "Dr. Yukiko Goda, Senior Team Leader, Lab for synaptic plasticity and connectivity" during the academic year 2016-17.

Student

Abhilash Sawant

Supervisor

Dr. Yukiko Goda

Declaration

I hereby declare that the matter embodied in the report titled "Understanding mechanisms responsible for the regulation of presynaptic strengths on a dendritic tree in rat hippocampal networks" are the results of the investigations carried out by me, Abhilash Sawant, at the Lab for synaptic plasticity and connectivity, RIKEN Brain Science Institute, Wako, Saitama, Japan under the supervision of Dr. Yukiko Goda and the same has not been submitted elsewhere for any other degree.

Student

Supervisor

Abhilash Sawant

Dr. Yukiko Goda

Abstract

Information transmission and storage in the brain is majoritively encoded by two main components of a neuron – axon and dendrite. Terminals and release sites of axons pair with spines on their dendritic counterparts forming synapses. Structurally, a synapse has two components – a presynaptic release site on an axon and a complementary postsynaptic receptive site on the spine of a dendrite. The release site is characterized by clusters of vesicles sitting at axonal compartments called boutons whereas the postsynaptic side is defined by a set of receptor/voltage-gated channels present on the corresponding spine surface. The strengths of these components, termed as pre and postsynaptic strengths, are stipulated mainly by the release probability of vesicles and number of receptors on the spine. These strengths are found to be fairly heterogeneous throughout the network. But the mechanisms by which these strengths are modified and regulated are not well discerned. Recently, another type of cells called astrocytes which previously were considered to be playing a supportive role are gaining recognition for their subtle involvement in synaptic transmission and strength regulation. Consequently, the view that astrocytes indeed form a communicative framework across different synapses for global strength regulation is emerging. The project broadly aims at understanding the mechanisms underlying this strength regulation in pyramidal hippocampal cells and the role of astrocytes in the same. In particular, we tested the hypothesis that astrocytes control the heterogeneity of presynaptic strengths of multiple synapses received by a postsynaptic neuron. We validated the use of an optical imaging approach using the FM 1-43 styryl dye for effectively monitoring the release probabilities of multiple synapses received by excitatory neurons. With this technique, we set out to examine the effects of pharmacological inhibition of astrocyte Calcium signaling in primary hippocampal cell cultures. All the experimental accomplishments and difficulties faced during the course of project are interpreted and discussed in this dissertation.

Contents

List of figures

List of tables

Acknowledgements

I would like to offer my heartfelt thanks to Dr. Yukiko Goda, RIKEN Brain Science Institute, Wako, Saitama for affording me the un-imaginable opportunity to carry out my 5th year BS-MS thesis project here. I will not forget to thank the Post-doctoral fellows in the lab, especially Thomas Chater and Peter Chipman, without whose patience, guidance and understanding, I would not have made it this far, especially the dissertation. I also remain thankful and grateful to fellow students and other Postdocs for their continuous guidance and providing a healthy research atmosphere. I would also like to thank the technicians for their consistent support in all the lab procedures and maintenance. I sincerely thank Dr. Nixon Abraham and Dr. Suhita Nadkarni, my guides at IISER, Pune for allowing me to come to RIKEN and carry out the project.

1. Introduction

1.1 Heterogeneity and variability in neuronal networks

Neurons can form connections with each other in order to encode various types of information. This connection, termed as synapse (Foster and Sherrington 1897) is the combination of presynaptic release and the post-synaptic receiver sites and a small space between them. The idea that neurons encode memories associated with learning dates back to the Croonian lecture given by Ramon Cajal in 1894 (Cajal, 1894). Due to various types of stimuli from the external world and requirement for robust responses via different sensory modalities, it is a natural consequence that the inputs and outputs of neurons are also diverse. This imposes a necessary condition on neurons that they should possess the ability to modulate their responses and tune the strengths of synapses in accordance with the required output. It opens a barrage of possibilities to accommodate for the diversity of activity at the circuit level via feedback loops, feedforward, lateral and recurrent inhibitory networks, functional columns etc. and at the molecular level by having robust expression of proteins, receptors, energy pumps, ion channels and ligands etc. (Stein et.al., 2005; Urban & tripathy, 2012). Indeed, this heterogeneity in the nervous system was seen differently by researchers at times. During initial stages of research in network modelling, the intrinsic variability of neurons was generally presumed to be a flaw by some and conjectured that it should be overcome by synaptic plasticity via learning (Lengler et.al. 2013). It is still difficult to provide a concrete explanation for the existence of heterogeneity but indeed there is building computational and theoretical evidence proving its efficiency over simple invariant and noise-free networks in terms of energy and speed of processing (Harris et. al., 2015; Mircea et. al., 2012). At the same time, models introducing external noise and mimicking physiological data by incorporating molecular properties of neurons like that of Crayfish and Squids (Douglas et. al., 1993; Wiesenfield and Moss, 1995; Moss, 2004) started emerging. Keeping all these factors constant, the system still exhibits some stochasticity at the level of electrical transmission across dendrites as well as chemical transmission at synapses. The former occurs by variable dendritic widths, spine shapes and neck sizes etc. (Ferrante et,. al., 2013; Anwar et. al., 2014; Hering &

Morgan, 2001) whereas the latter mainly depends on the probability of vesicular release at synapses. The mechanism of vesicular release at synapses is inherently stochastic. This feature was first demonstrated in peripheral synapses such as that of frog neuromuscular junction (NMJ) - quantal vesicle release detected in the form of focal mini-EPSPs (miniature excitatory postsynaptic potentials) at the end plate (Castillo & Katz, 1954). However, the reliability of release per action potential further reduces in mammalian central synapses as the number of active zones drops down significantly (Sorra and Harris, 1993; Schikorsk and Stevens, 1997). Studies in CA3-CA1 synapses of hippocampal slices and pyramidal neurons in cortical slices show high failure rate of neurotransmitter release per action potential (Raastad et.al., 1992; Allen and Stevens, 1994; Wang and Stevens, 1994; Wang and Stevens, 1995). Apart from this, the degree of stochasticity of neurotransmitter release varies from synapse to synapse (Allen and Stevens, 1994; Hessler et. al., 1993, Rosenmund et. al., 1993, Malinow et. al., 1994, Murthy et. al., 1997). Thus, it is apparent that evolution has shaped the brain in such a way that it maximizes information processing by the presence of diverse molecular mechanisms, functional units and modes of release.

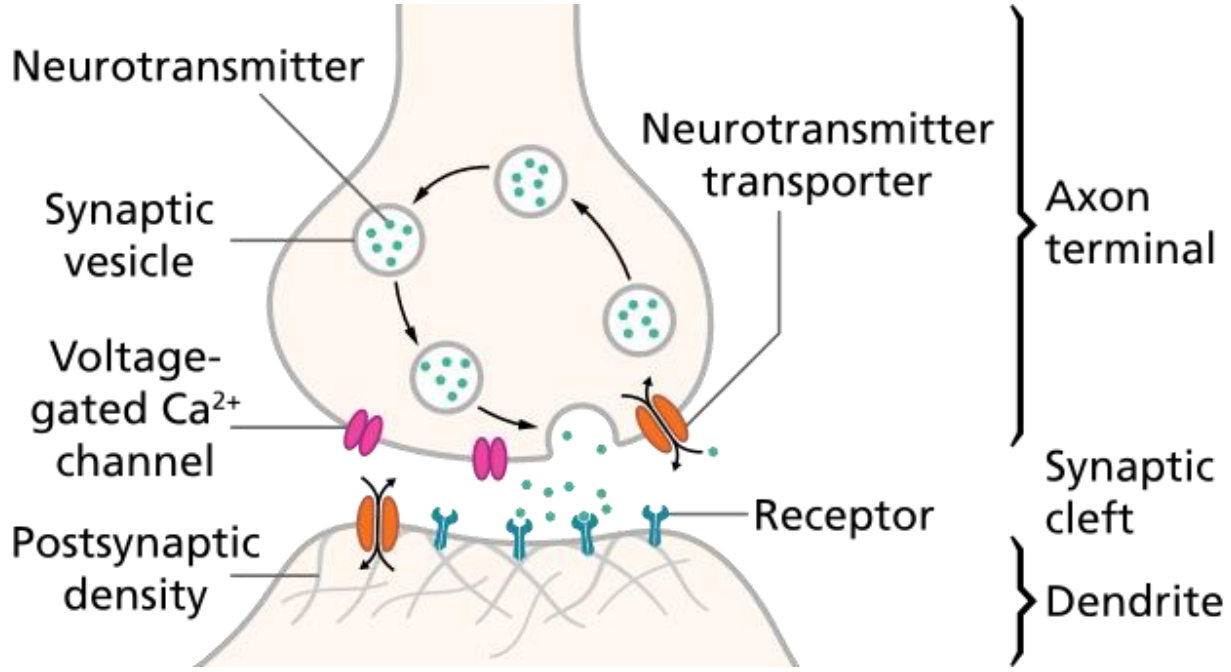

Figure 1. Schematic depicting the Calcium-dependent vesicular neurotransmitter release cycle.

Image source: Thomas Splettstoesser

1.2 Mechanism of presynaptic release and concept of release probability Pr

The mechanism of signal transmission across axons is well studied and characterized. Action potential is generated in the soma, travels through the axon (Purves et. al. 2001), and arrives at release sites called boutons. These boutons comprise of pools of small packets called vesicles, which contain neurotransmitter. Some of them are docked at the release site termed as the Active Zone (AZ) (Thomas Sudhof, 2012; Stigloher et. Al., 2011; Siksou et. al., 2009; Mukherjee et. al., 2010; Hallerman et. al., 2010) and form the Readily Releasable Pool (RRP) (Rosenmund and Stevens, 1996). Arrival of an action potential triggers the opening of Voltage Gated Calcium Channels (VGCCs) around the AZ and triggers Calcium-dependent interaction of a protein complex called SNAP-SNARE complex which is the release machinery of vesicles (Rizo et. al., 2015). This whole process is termed as exocytosis (Sudhof T.C., 2004; Katz, 1969; Gandhi & Stevens, 2003; Goda & Sudhof, 1997) and is followed by reuptake of membrane proteins and transport machinery (for budding, invagination, fission and transport) back into vesicles by a mechanism called endocytosis (Sudhof T.C., 2004; He & Wu, 2007; Galli & Haucke, 2001). However, an action potential arrival does not always elicit vesicular release and hence, the process is stochastic. The degree of stochasticity varies across synapses and this aspect is associated with the probability of release Pr. It has been revealed by a number of studies in hippocampal slices and dissociated cultures that the chances of vesicular release increase with higher number of docked vesicles in a bouton and thus, Pr is correlated with the size of RRP (Branco & Staras, 2009; Staras et.al., 2008).

1.3 Existing mechanisms underlying Pr regulation

Given that this heterogeneity exists across synapses, the exact mechanisms underlying the regulation of Pr are under intense scrutiny. It is necessary to outline the mechanisms contributing to the efficacy of vesicle release process, heterogeneity, and its regulation to gain a better understanding of its implications on information processing. Nevertheless, further focus of this report will be on the mechanisms underlying this regulation and the possible involvement of astrocytes. Recent views on Pr regulation point towards participation of Hebbian and homeostatic plasticity mechanisms as well

as activity history and feedback regulation from the postsynapse (Branco & Staras, 2009; Staras et.al., 2008).The components of presynapse, which can be influenced under regulation, at least include the number of Calcium channels and vesicles available for release. It is known that the release probability is modulated by long-term plasticity and long-term potentiation (LTP) increases the reliability of release, i.e., the Pr (Dobrunz and Stevens, 1996; Dobrunz, 2002; Emptage et. al., 2003) This suggests that long-term Hebbian plasticity of dendritic spines might communicate via retrograde messengers to the presynapse for tuning its strength of release. Several lipid-based molecules, gases, peptides, neurotransmitters, growth factors, and secretory proteins have been identified as messengers (Carey et.al., 2009). Role of synaptic homeostasis is also implicated in regulating Pr – halting action potential generation and blocking glutamate receptors in hippocampal cultures increases the frequency of miniature excitatory postsynaptic currents and neuronal excitability. This also reflects an overall increase in Pr (Bacci et. al., 2001; Thiagrajan et. al., 2005; Thiagrajan et.al., 2002). Studies on cortical cultures (Wierenga et. al., 2006) and hippocampal organotypic slice cultures (Galante et.al., 2001) also show similar effects on presynaptic by changes in AZ size, number of docked vesicles (Murthy et.al. 2001), and synaptic vesicle recycling. Short-term activity also influences Pr by dynamically changing the various factors of release like vesicle recycling rates, neurotransmitter packing efficiency, Calcium buffering, vesicle pool size etc.(Zucker and Regehr, 2002).

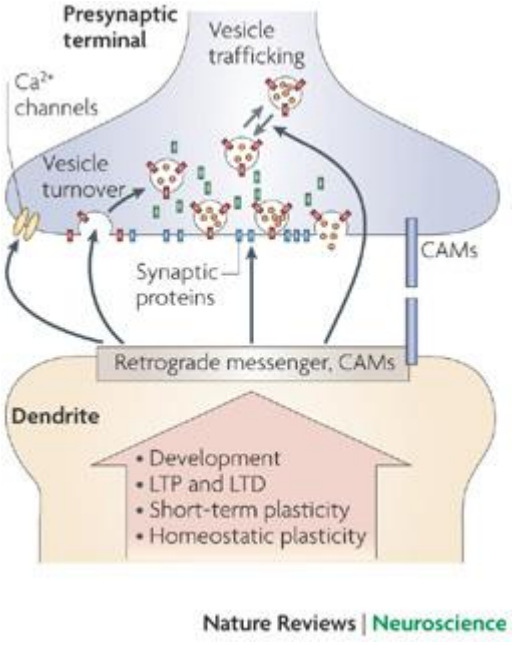

Figure 2. Depicts a schematic representation of feedback mechanisms underlying Pr regulation. Source: (Branco & Staras 2009)

1.4 Astrocytes as a mode of synaptic strength regulation

Astrocytes, a class of glial cells, were known to have only a supportive role in the brain

via providing nutrition and taking part in regulatory functions necessary for synaptic transmission for several decades. These cells are found to wrap around synapses by extending perisynaptic processes and form the third component of a tripartite synapse (Araque et.al., 1999). This concept was established based on the emerging evidence of a bi-directional communication between astrocytes and synapses (Perea et.al., 2009). It was long back established that astrocytes responded to neuronal stimulation by reflecting the changes in Potassium concentration ([K+]) first in amphibian glial cells (Orkand et.al., 1966) followed by mammalian glia (futamachi and Pedley, 1976; Miller et.al., 1977; Roitbak AI & Fanardjian VV, 1981). Astrocytes are also known for their homeostatic role in rapid clearance of glutamate on release from neurons at synapses via Excitatory Amino Acid Transporters (EAATs) like GLT-1 and GLAST expressed on astrocyte membrane (Bergles DE & Jahr CE, 1997; Diamond JS & Jahr CE, 2000; Danbolt NC, 2001; Diamond JS, 2005). This clearance of glutamate was later associated with generation of Calcium transients, NMDA receptor activation and synaptic plasticity (Jensen et.al., 2002; Marvin et.al., 2013). The conventional view gradually shifted as more and more participation of astrocytes in synaptic transmission and plasticity via neurotransmitter sensory and release mechanisms Araque et.al., 2014; Min et.al. 2012). Astrocytic Calcium transients have been implicated during and after synaptic transmission via various pathways (Bazargani & David Attwell, 2016).

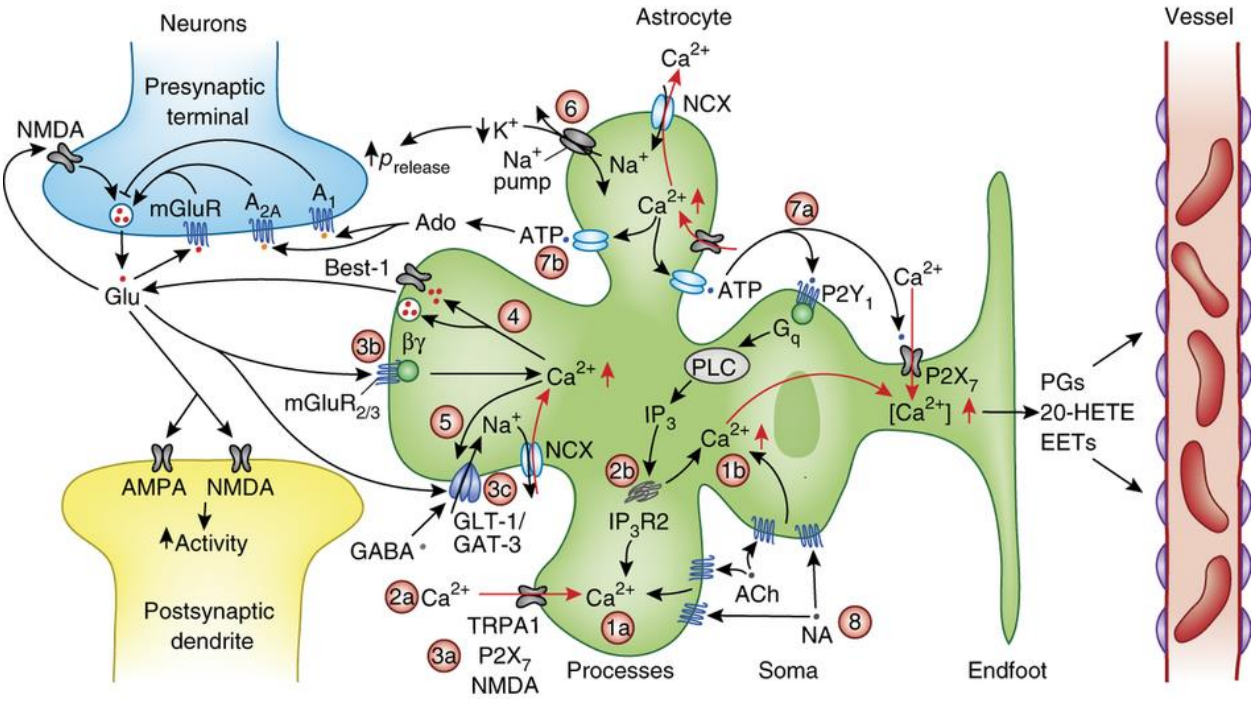

Figure source: Bazargani &

Figure 3. Atwell 2016. A schematic representing the pathways and channels as sources of triggering Calcium release from astrocytic internal stores.

In hippocampus, astrocytic gliotransmitter dependent LTP, depression and heterosynaptic long-term depression (LTD) has been demonstrated (Pascual et.al., 2005; Serrano et.al., 2006; Zhang et.al., 2003). This heterosynaptic LTP is presynaptically modulated – Pr of the heterosynapse (synapse between the neuron other than which is being stimulated but sharing the same postsynaptic neuron) is downregulated by inhibitory gliotransmitter ATP from astrocytic process. Recent studies show that this release is triggered by astrocytic Calcium signaling initiated by glutamate released from the homosynapse (synapse between the neuron which is being stimulated and the one which is postsynaptic to it) during a tetanic stimulus. Thus, astrocytes help balance the synaptic composition on a neuron through counterbalancing a potentiated input by depressing the neighboring one (Zhang et.al., 2003; Chen et.al., 2013). Further study show that this astrocyte Calcium signaling-dependent mechanism exists at the level of basal strengths as well by an NMDAR-dependent mechanism (Letellier et.al., 2016). This paper addressed this the regulatory aspect of astrocytes in a three neuron setup – two convergent inputs on a target neuron. They stimulated the inputs corresponding to homosynapse and heterosynapse with a paired-pulse and

measured Paired Pulse ratios (PPRs) in hippocampal cultures (data shown) and acute brain slices (data not shown). Paired Pulse Ratio is a measure of Pr of a synapse which is measured by the ratio of amplitude of the second pulse to that of the first on stimulation by two action potentials. In pharmacological conditions of NMDAR channel and L-type Voltage Gated Calcium Channel (VGCC) blockade, the PPRs of both inputs correlated and became similar. Thus, astrocytes tend to maintain the heterogeneity of synapses at least in a heterosynaptic setup. Whether this regulatory mechanism exists at a global level is unknown. This project attempts at probing this aspect of the regulation and gauge the extent to which it exists in a network. Since astrocytes modulate synaptic strengths or plasticity of a synapse presynaptically, Pr is presumed to be directly affected by this regulation.

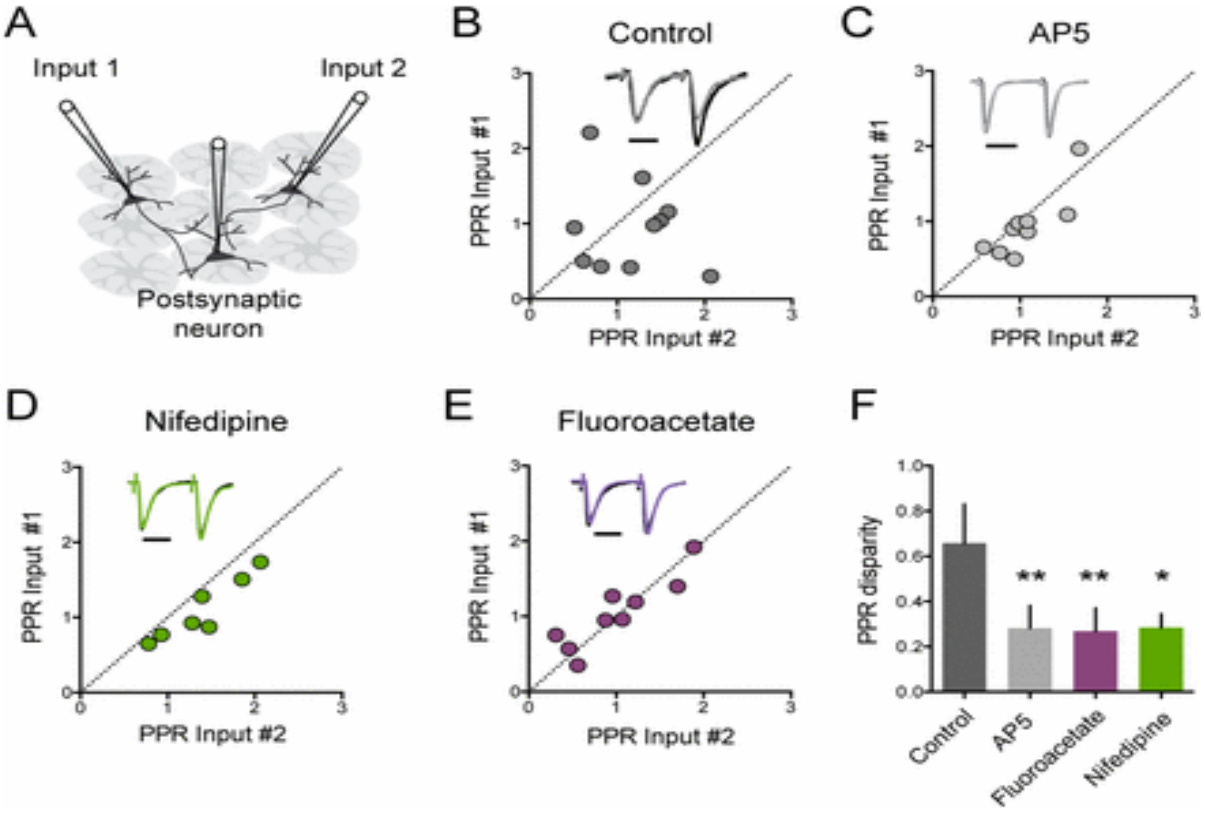

Figure 4. NMDAR and L-VGCCs are necessary for decorrelation of presynaptic strengths of convergent

inputs (A) Experimental scheme for comparing two independent convergent inputs. Monosynaptic currents recorded in the postsynaptic neuron by stimulating each of the two presynaptic neurons are compared. (B–E) Scatter plots and average traces from representative cells comparing basal PPR of the two independent inputs for control (n = 10 cells, r2 = 0.04, P = 0.5834), AP5 (n = 9 cells, r2 = 0.6960, **P = 0.0052), nifedipine (n = 7 cells, r2 = 0.88, ***P = 0.0016), and fluoroacetate (n = 9 cells, r2 = 0.81, **P = 0.001). (F) Summary of the average basal PPR difference for the same conditions (one-way ANOVA followed by Holm–Sidak's multiple comparison test, *P < 0.05, **P < 0.01). Data are expressed as mean ± SEM. (Figure taken from Letellier et. al., 2016)

1.5 Methodological approach

For wide-scale monitoring of synaptic strengths, an optical approach is beneficial rather than a temporally precise but spatially restricted electrophysiological approach since the temporal component is not that strict in this case as the analysis requires a population measurement of basal presynaptic strengths and no synapse-specific plasticity-induction over time. We approach the problem by applying pharmacological drugs and compromise astrocytic Calcium dynamics while optically monitoring presynaptic strengths. FM 1-43 dye is a suitable presynaptic tracer labeling technique for this approach (Ryan et.al., 1997; Harata et.al., 2001). As discussed before, RRP size is directly correlated with Pr of a synapse and using a stimulation paradigm that labels RRP with FM 1-43 dye is an indirect measure of presynaptic strength. Firstly, I explore and test various approaches for labeling and quantifying pre and postsynaptic strengths. Then I decide to chose FM 1-43 dye as a measure for monitoring presynaptic strengths due to previous evidence (Tokuoka and Goda, 2008). Initial step was to test the sensitivity of FM dye towards RRP sizes in different external Calcium concentrations as presynaptic Calcium influx is linked to the effective RRP size and hence, the Pr (Thanawala et.al., 2013). The project plan then moved on towards application of NMDAR channel blocker as means of disrupting Calcium-dependent signaling by astrocytes and hence, blocking the Pr regulation. As time progressed, I encountered some technical difficulties during the experiments and hence, invest time in troubleshooting the problems. All the tests done, progress made, troubles encountered, and measures taken to solve them are addressed in this dissertation. During the course of project, critical thinking on the problem led to the development of many different possible approaches to tackle the research problem and are illustrated in the future

directions.

2. Materials & Methods:

2.1 FM 1-43 styryl dye:

FM 1-43 is a styryl amphipathic fluorescent dye which can be used for labeling of recycling synaptic vesicles. It normally shows very low fluorescence in aqueous solutions and increases upto 100-fold when it's lipophilic part binds to the cell membrane. After exocytosis, equivalent amount of fused membrane is integrated into vesicles by endocytosis, thus, enabling visualization of presynaptic strengths as a measure of the amount of membrane-associated fluorescence signal uptake. The rest of the membrane which is bound by FM 1-43 is washed off by Advasep-7, a chelating agent for the dye. By using a field stimulation paradigm of 40 Action Potentials (APs) at 20Hz (20Volts with a pulse duration of 1 millisecond and electrode separation of approximately 1 centimeter), we attempt to make vesicles associated with the release probability undergo the exo-endocytotic cycle. After washing off in Extracellular Buffer Solution [EBS] for 10 minutes, the neurons are stimulated at 600APs, 20Hz [unloading paradigm] for avoiding the count of endocytosis due to spontaneous release. Imaging commences 15 seconds prior to the unloading paradigm with an interval of 2 seconds and ends 15 seconds after it. The following figure (Tokuoka & Goda, 2008) depicts the chronology of steps:

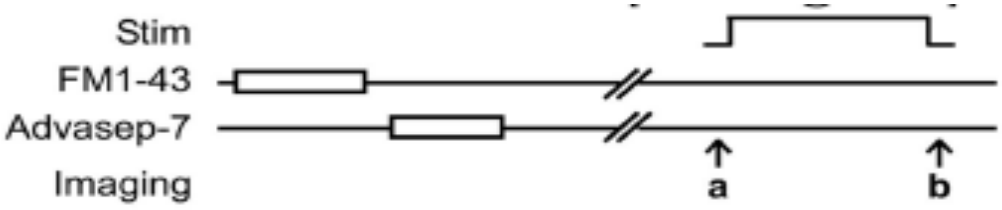

Figure 5. A schematic representing the course of a typical FM 1-43 labeling experiment. **a** and **b** represent the start and end-points of imaging.

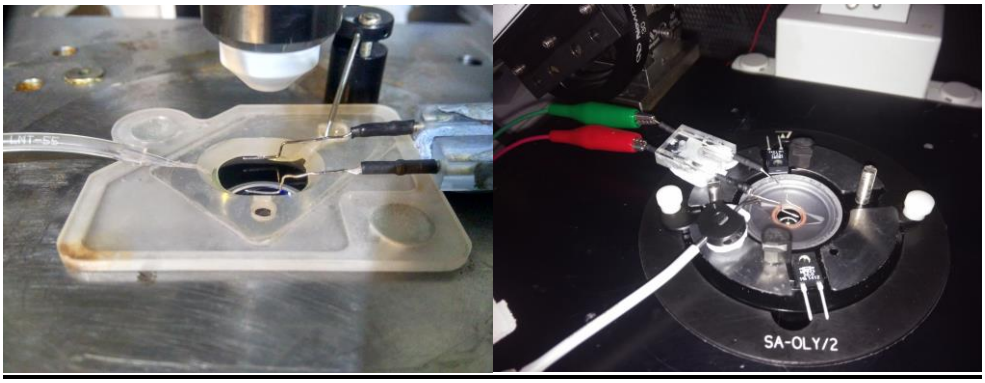

Figure 6. 2 types of chambers used in experiments.

2.2 Cell Culture:

Dissociated cultures of hippocampal neurons were kindly provided by Prof. Yukiko Goda throughout the experiments. Neurons were cultured on top of a monolayer of conditioned astrocytes. Sets of experiments were done in the presence of 6-cyano-7-nitroquinoxaline-2,3-dione (CNQX-10μM) and Picrotoxin (100μM).

2.3 Extracellular Buffer Solution [EBS]:

The normal EBS consisted of (in mM]) 137 NaCl, 5 KCl, 10 D-Glucose, 5 HEPES (pH 7.3), 2 $CaCl_2$, 2 $MgCl_2$, 0.01 CNQX at ~300 mOsm. Advasep-7 was made in wash EBS (0.1mM $CaCl_2$ in EBS) which was further used for washing off the dye. Solutions for testing Calcium sensitivity were made up in EBS with varying [Ca^{2+}]. FM 1-43 dye (Molecular Probes Catalog number: T35356) was made up in CNQX, Picrotoxin containing EBS at a concentration of 10μM.

2.4 Fluo-4 AM:

Fluo-4 is a Calcium dye used in screening of Calcium associated molecules. The AM variant (Molecular probes Catalog number: F14201) is cell permeable and can be used in monitoring in-cell spatial dynamics of Calcium signaling as the cell undergoes fluctuations in Calcium concentration. Excitation frequency is 488nm and emission at 520nm. Fluorescence intensity increases >100 fold on binding to Ca^{2+}. Cover slips are incubated in 10μM dye containing EBS and incubated at room temperature for 20 minutes. Then they are transferred to fresh EBS and taken under microscope for

measuring fluorescence signal. Timelapse imaging was done at 2 Hz for different total times.

2.5 Imaging:

Images were captured with a cooled CCD camera attached to an IX71 microscope (Olympus) with an X40 water immersion lens, a 470/50 nm excitation filter and a 545/75 emission filter and Metamorph software (Universal imaging corporation). Neutral density filters were engaged to reduce the excitation light intensity to 25%.

2.6 Immunostaining

In all experiments, cells were permeabilized after fixation (with 4% paraformaldehyde) with solution A for 15 minutes and blocked in solution B/serum for 1 hour. Primary antibodies were added in solution A and incubated for 1 hour. After three washes in solution B spaced by 10 minutes, neurons were incubated with secondary fluorescently conjugated antibodies for 30 min-1 hour. After 3 washes with solution B spaced by 10 minutes each, the coverslip was mounted on glass slides using vecta shield. All procedures were carried out at room temperature. The composition of solutions is as follows –

Fixation - 4% v/v of Paraformaldehyde in Phosphate Buffered Saline (PBS)

Solution A – 0.2 M Na_2HPO_4 + NaH_2PO_4 at pH 7.3, 10% (v/v) triton-X100, 2 M NaCl, goat serum and dH_2O.

Solution B – 0.2 M Na_2HPO_4 + NaH_2PO_4 at pH 7.3, 2 M NaCl, dH_2O.

Solution B/serum – 0.2 M Na_2HPO_4 + NaH_2PO_4 at pH 7.3, 2 M NaCl, goat serum and dH_2O.

3. Analytical methods:

3.1 For measurement of synaptic strengths of stained boutons by FM 1-43 dye:

First and the last planes from time lapse taken during unloading stimulation were extracted by using Metamorph imaging software (Metamorph Corporation) and checked

for destained synapses. The synapses which underwent destaining were selected and puncta intensities were measured by assigning (9µm x 9µm) boxes over synapses for both planes by using Openview software kindly provided to the lab by Dr. Noam Ziv (Israel Institute of Technology). The intensities of puncta from last plane was then subtracted from corresponding synapses of the first and this value was used as "strength of a synapse". The sampling was done by taking around hundred synapses per cell and n number of 4-5 cells per concentration. An example image of analysis is shown. ImageJ was used to crop images of last plane which shifted during stimulation and overlay with the first plane. Intensities were then plotted with the frequency of synapses as histograms using Microsoft excel and then fitted into Gaussian functions using Graphpad Prism and plotted.

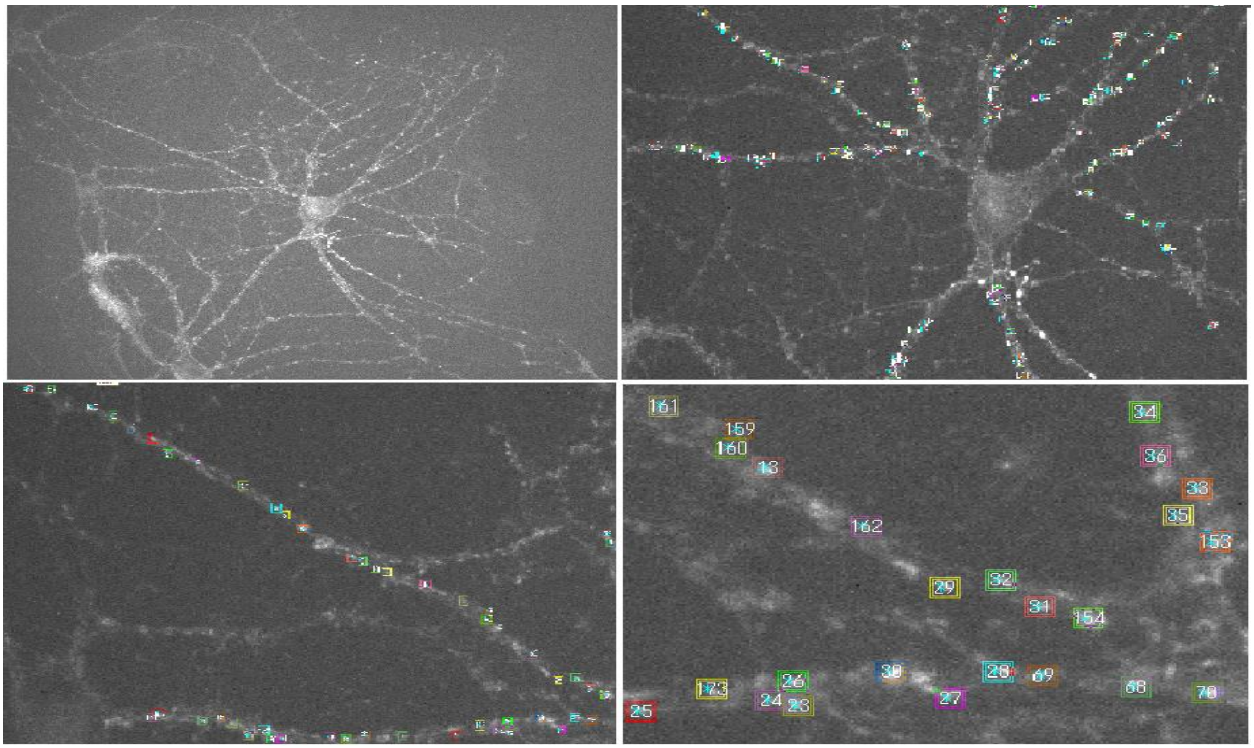

Figure 7. An example image of analysis is shown. (Left top) - raw image. (Right top) – assigned puncta. (Bottom) – zoomed in versions of top. Boxes assigned by Openview.

3.2 <u>For measurement of Calcium dye responses by Fluo4-AM:</u>

Regions of interest were marked on the time lapses and optical signal was analyzed by using Metamorph imaging software. Integrated intensity values were exported to Graphpad Prism and plotted as a function of the plane number.

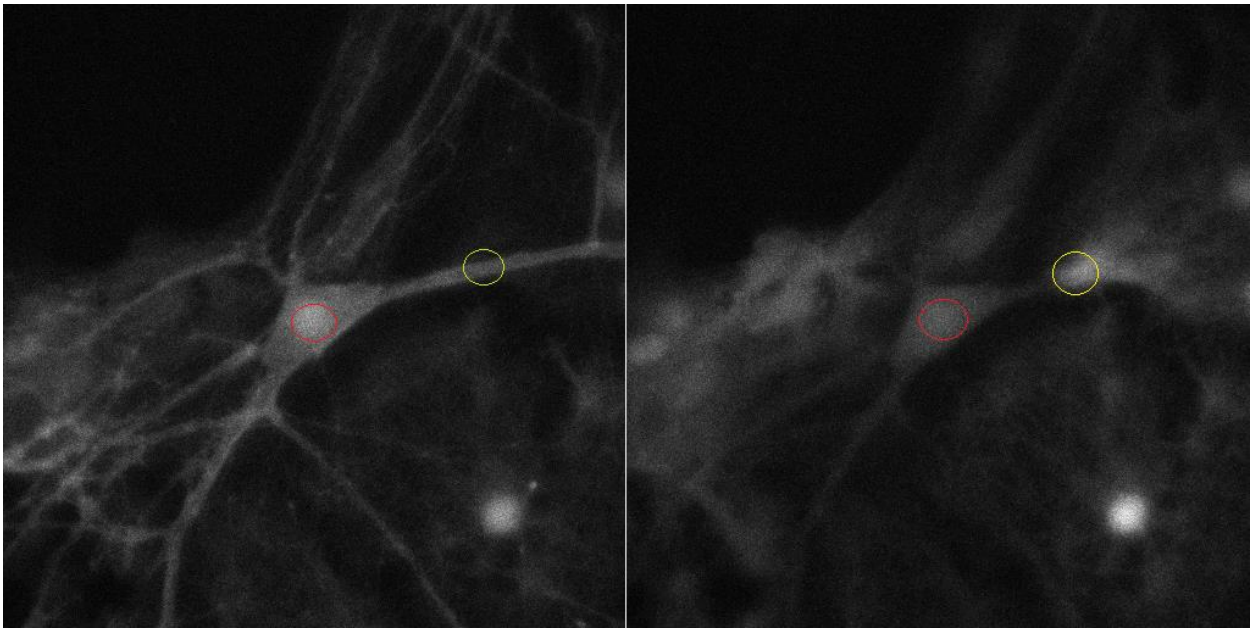

Figure 8. An example image of analysis is shown. Red ROI is for monitoring soma Calcium dynamics and yellow ROI for dendrite and astrocyte. (Left) A neuron during firing and (right) astrocyte depolarization near the dendrite ROI.

4. Results and Discussion:

In the first 4 sections, I describe the various approaches used for optimization of techniques and screened for potential candidates which could be used to quantify presynaptic strengths. Then I move on to FM 1-43 dye validation and the experimental condition of AP-5 in sections 5 and 6. Section 7 focusses on the problems faced during FM 1-43 labeling experiments and the troubleshooting steps taken to tackle the problem. Finally, I describe a side experiment of Calcium imaging using Fluo4-AM which stemmed from the troubleshooting process.

4.1 Optimizing dilution for Alexa 550 GluA2/3 Oyster Antibody to be used as a quantifying approach for postsynaptic strengths

The Antibody was tested for different dilutions – 1:50, 1:100 and 1:200 ratios of

Antibody to Extracellular Buffer Solution for labeling the GluA2/3 subunits of AMPA receptors. Criteria for optimum dilution was set to be sufficient visibility of signal but not high intensities because of background increase. Example raw data is shown.

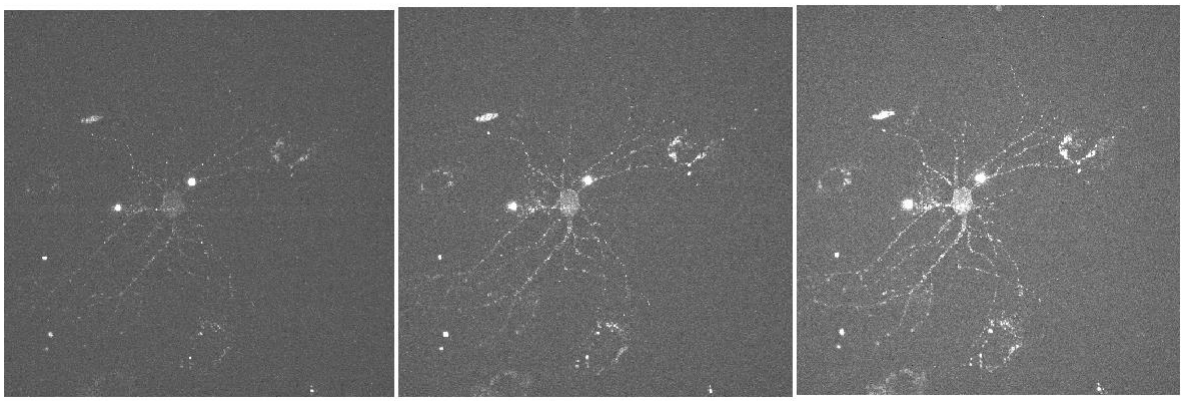

Figure 9. 1:50 1:100 1:200

Dilutions of antibodies and corresponding images at excitation wavelength 550nm.

1:100 dilution was chosen as the optimal concentration of the Antibody. The experiment was repeated for 3 samples and images were taken at 3 different light exposure times of image capture – 10,30,50 milliseconds.

4.2 Immunolabeling of dissociated cultures as a possible approach for quantifying presynaptic strengths

I performed immunostaining of dissociated cultures by primary and secondary antibody labeling. A wide range of antibodies were tested and fixed cells were stained for imaging. Here I show raw data corresponding to Microtubule Associated Protein (MAP)-2 antibody staining and synaptotagmin-I labeling on axons. The MAP-2 staining labels whole neuronal morphology to visualize the postsynaptic neuron and can be evinced clearly from the data. However, syt-I punctate staining labels most of the synapses on a single axon. What I required is strengths distributed on a dendritic tree coming from different inputs but the efficiency of antibody labeling and possible measurement of non-synaptic puncta (autofluorescence) due to non-specific antibody binding introduces an an err factor in measuring presynaptic strengths.

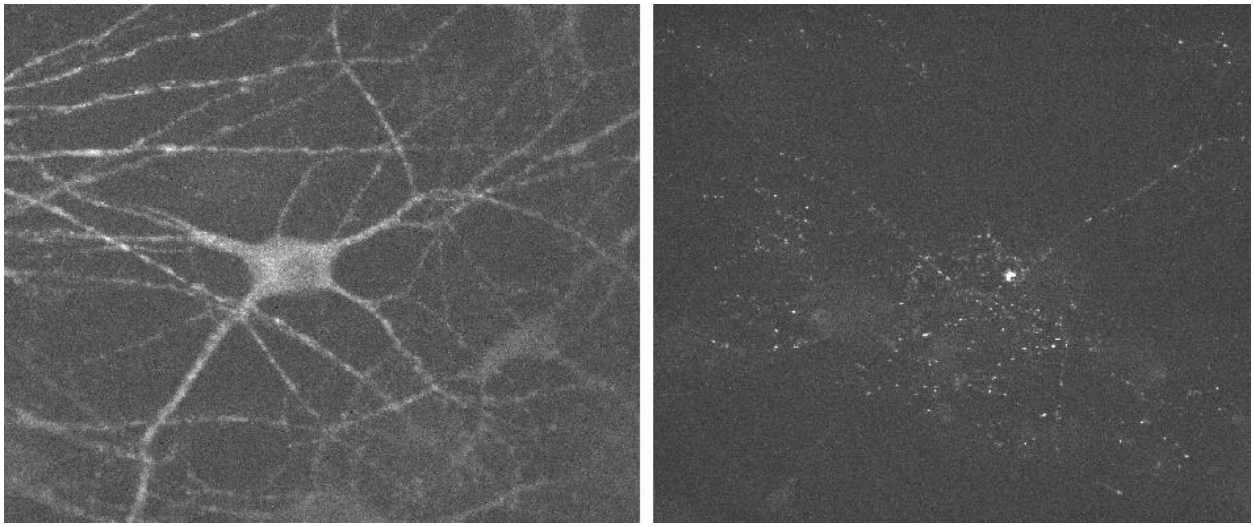

Figure 10. Image (left) - MAP2 staining of neuron and (right) – synaptotagmin-I puncta spread across in the middle and an axon extending towards right.

4.3 VGluT-pHluorin signal test by 45mM K^+ depolarization

Day in vitro (DiV) 7 cells were transfected with VGlutI-pHluorin construct by Lipofectamine 2000 transfection method. 3 coverslips were taken for experiment and incubated with 45mM K^+ solution to visualize the extent of depolarization and compare. The conditions were as follows – A.) 1 min incubation, 2.) 5 min incubation and 3.) Control – 2mM K^+ EBS incubation for 5 min. The signal in 5 min incubation was slightly stronger than that of 1 min and control. There was however, no difference noticed in 1 min incubation and control. This could be explained by reacidification kinetics of the phluorin. Vglut1 remains quenched inside of vesicles (pH 5.5) but is fluorescent upon release into the extracellular solution (pH 7.3). Later, the vesicles are endocytosed and reacidified back with a time constant of about 10-15 and 5 seconds respectively. Imaging was done pre and post 3 mins of incubation so no signal was expected and observed. The signal in 5 min incubation was probably debris from excitotoxicity. Ongoing experiments are being done with simultaneous imaging during stimulation at different conditions to monitor astrocyte-dependence of presynaptic strengths on a single axon.

4.4 Synaptophysin-GCamp3 and mcherry transfections for optimizing transfection efficiency and signal detection.

The method used for transfecting plasmids into neurons was the Calcium phosphate transfection method. This method was preferred over the widely used method of Lipofectamine transfection as it was evinced by a series of experiments at Dr. Volker Haucke's (FMP, Berlin) lab that Lipofectamine method interferes with the rates of vesicle recycling and hence, would disrupt the refilling of RRP. Since it can potentially hamper endocytosis which can inflict errors in the 45 second time interval for vesicle recycling, the method of transfection was changed to Calcium Phosphate. Neurons of age DiV 7-9 were transfected with the following constructs for optimizing Calcium Phosphate transfection protocol – A.) Synaptophysin-Gcamp3 + mcherry co-transfection. B.) VGlut-pHluorin + mcherry co-transfection C.) mcherry alone. Each combination of constructs was repeated with 2 different plasmid amounts. For A.) and B.), 0.5µg of each construct and 1µg of each were tested. For C.) 0.5, 1 and 2µg of constructs were taken. Efficiency of transfection peaked for lower plasmid concentrations. In case of mcherry, efficiency for 0.5 and 1 µg DNA was similar. Therefore, a total of 0.5µg of plasmid for single transfection and 1µg of plasmid for double transfection was concluded to be optimal.

4.5 Validation of the use of FM 1-43 styryl dye for monitoring RRP size

FM 1-43 dye application at 40APs, 20Hz labels a fraction of vesicles of the RRP. Since this fraction or the release probability is itself dependent on Calcium concentration, the first step is to verify the sensitivity of the dye by varying external [Ca^{2+}] – 0.8, 1.0, 2.0, 5.0, 7.5 and 10.0 mM. Figures are related to 2 conditions – 1.) CNQX only (AMPA/Kainate receptor antagonist used for blocking recurrent excitation). 2.) CNQX+AP5.

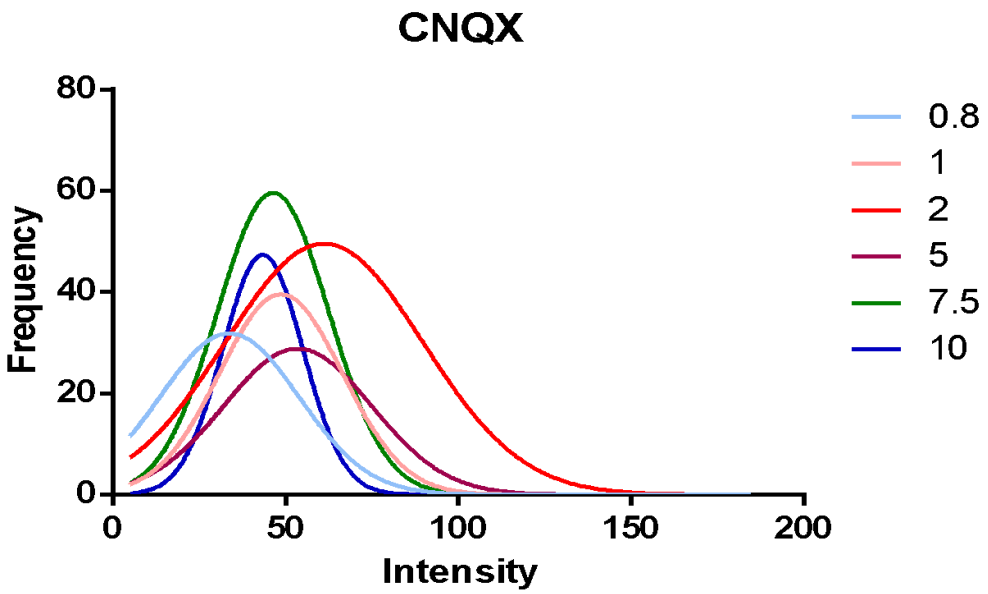

In all images, intensity corresponds to the value attained by described analytical method for measuring presynaptic strengths. Frequency is the number of occurrences.

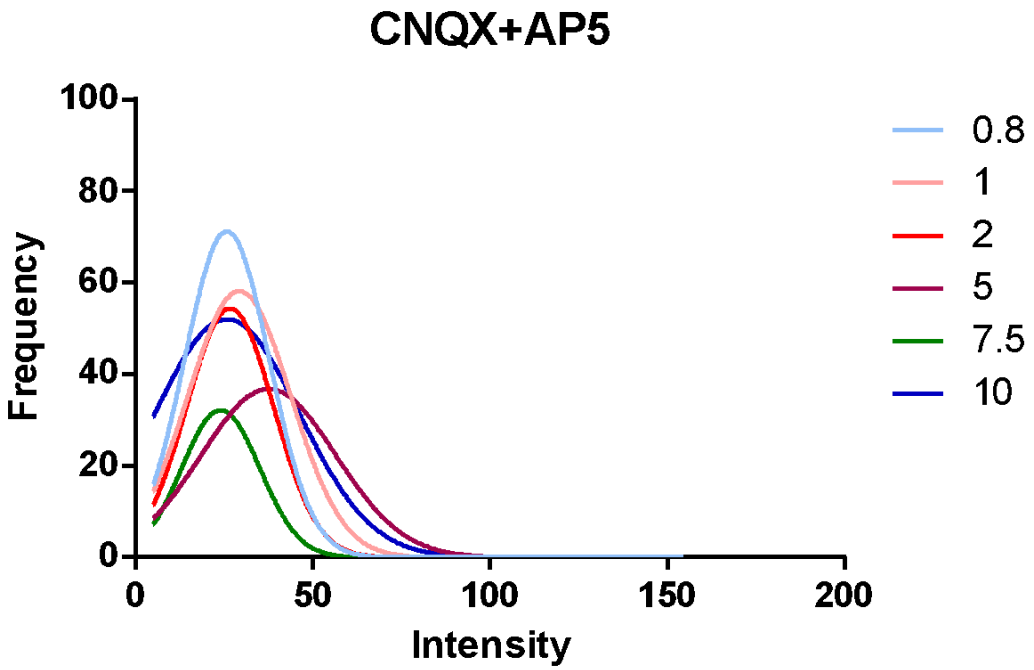

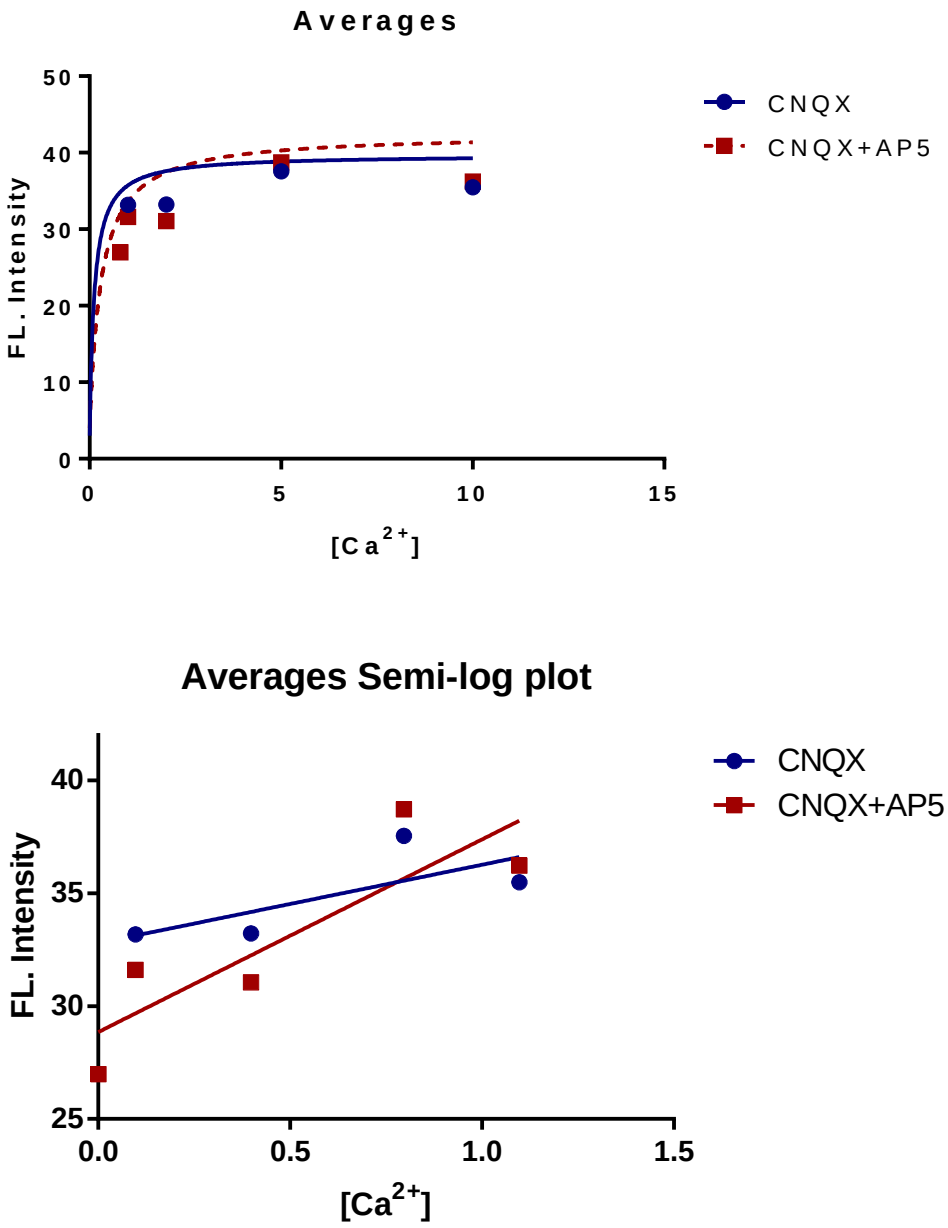

Figure 11: Intensities of presynaptic strengths plotted by fitting the frequency histograms. (Top) Control condition. (Middle) Experimental condition – CNQX + AP5. (Bottom) – Linear and semi-log plot of averages versus Calcium concentration for CNQX and CNQX+AP5 experiments.

The mean fluorescent values and number of synapses and coverslips for both the conditions are as follows – (Since the N number for 7.5mM Calcium were very less as compared to others, they were excluded out of the analysis)

A.) CNQX only. **Table 1 -**

Calcium Concentration	Mean Intensity	n (Coverslip),N (synapses)
0.8	30.78	2, 135
1	33.81	4, 300
2	33.22	4, 236
5	37.55	3, 482
10.0	35.49	4, 284

B.) CNQX + AP5. **Table 2 -**

Calcium Concentration	Mean Intensity	n (Coverslip),N (synapses)
0.8	26.99	4, 435
1	31.61	4, 431
2	31.06	3, 362
5	38.71	3, 348
10.0	36.23	3, 525

In both plots, the mean of the distributions for [Ca^{2+}] – 0.8, 1 and 2 appear to be increasing linearly but the trend disappears onwards. There can be a number of reasons for this inconsistency. Although optical imaging is less arduous, there are some caveats associated with it. First of all, the experiments involve mild stimulation initially [40APs, 20Hz, 20V] followed by a heavy unloading stimulation (600APs, 20Hz, 20V). The health of cells sometimes fail to keep up (seen by bursting of cells under phase contrast microscope) resulting in reduced de-staining towards the end of the experiment. Second, the age of the cells during these experiments was DIV 23-27. Relatively old/mature cells wear out due to long term growth in an artificial environment and are unreliable for experiments. Sometimes, an inhibitory neuron can get recruited for analysis under the presumption of a pyramidal cell. The analysis is restricted to pyramidal neurons only because sensitivity of neurotransmitter release to external Ca2+ can vary across neuronal types (Hefft and

Jonas, 2005). Therefore, the data corresponds to putative pyramidal neurons. Nevertheless, the variation implies a certain degree of sensitivity towards changing [Ca^{2+}].

4.6 Comparison between strength disparity in the presence and absence of NMDAR antagonist AP5:

A first hand approach towards testing an NMDAR-dependent change in the disparity of release probabilities is to look at the variance of distributions of synapses by blocking NMDAR function. The control condition contains only CNQX and not AP5, which (AP5) is an NMDAR antagonist and inhibits the glutamate binding site of NMDA receptors by competitively binding to them. We again test this for a range of Calcium concentrations – 0.8, 1.0, 2.0, 5.0, 7.5 & 10.0 mM. Figures depict the data.

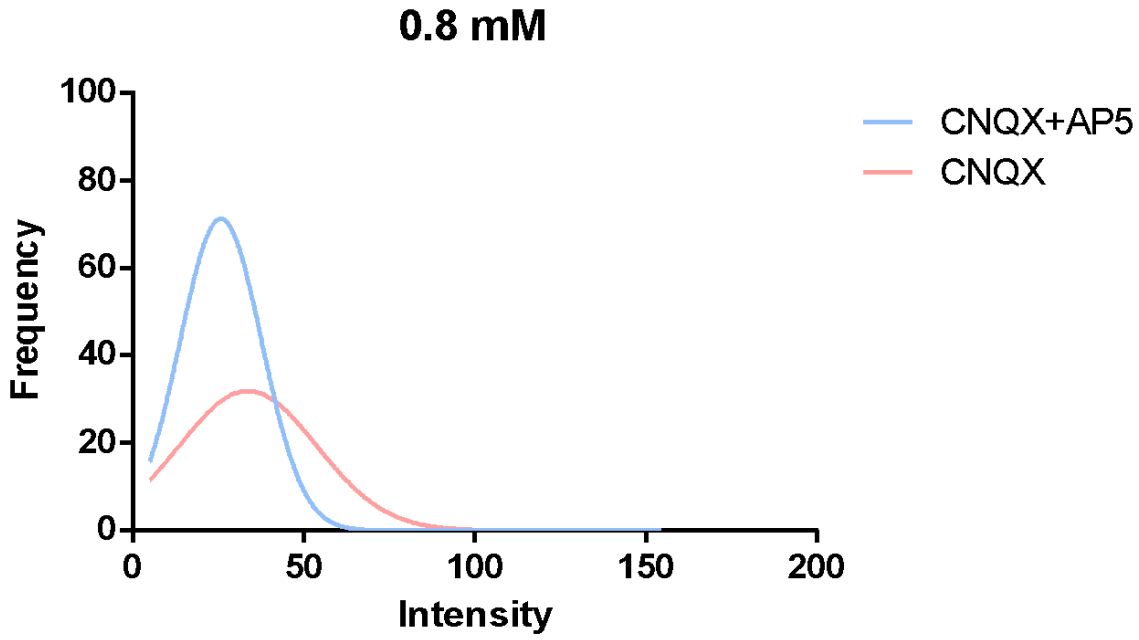

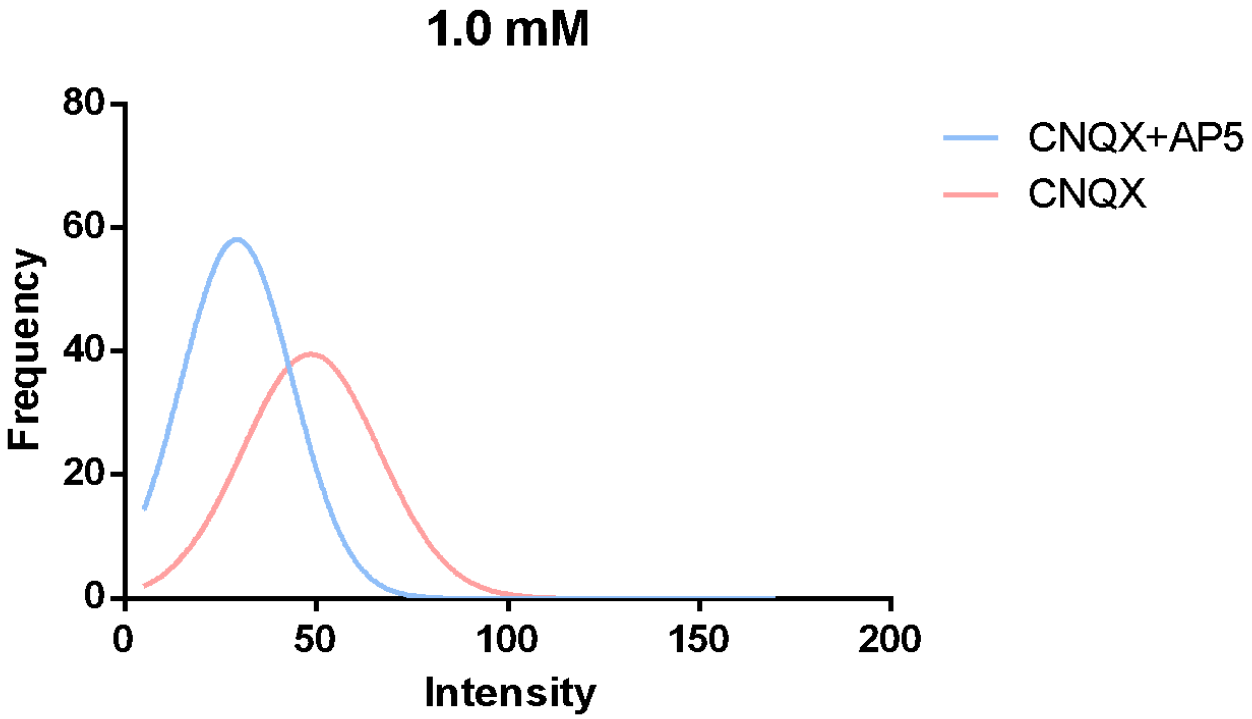
1.0 mM
Frequency
80
60
40
20
0
0
50
100
150
200
Intensity
CNQX+AP5
CNQX

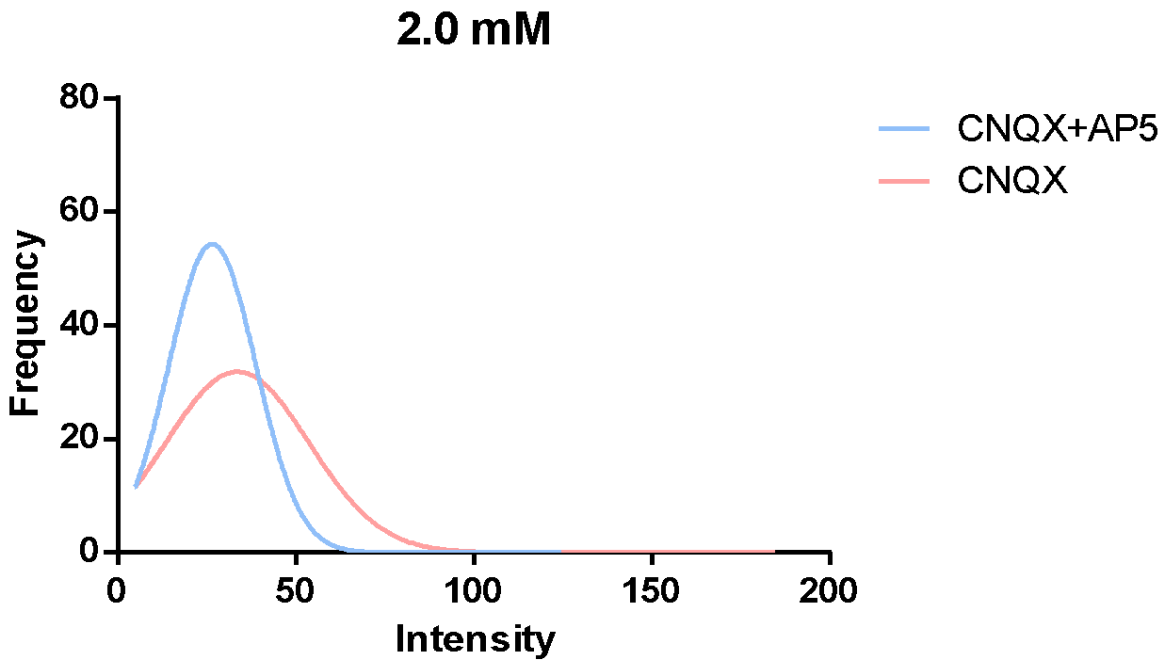
2.0 mM
Frequency
80
60
40
20
0
0
50
100
150
200
Intensity
CNQX+AP5
CNQX

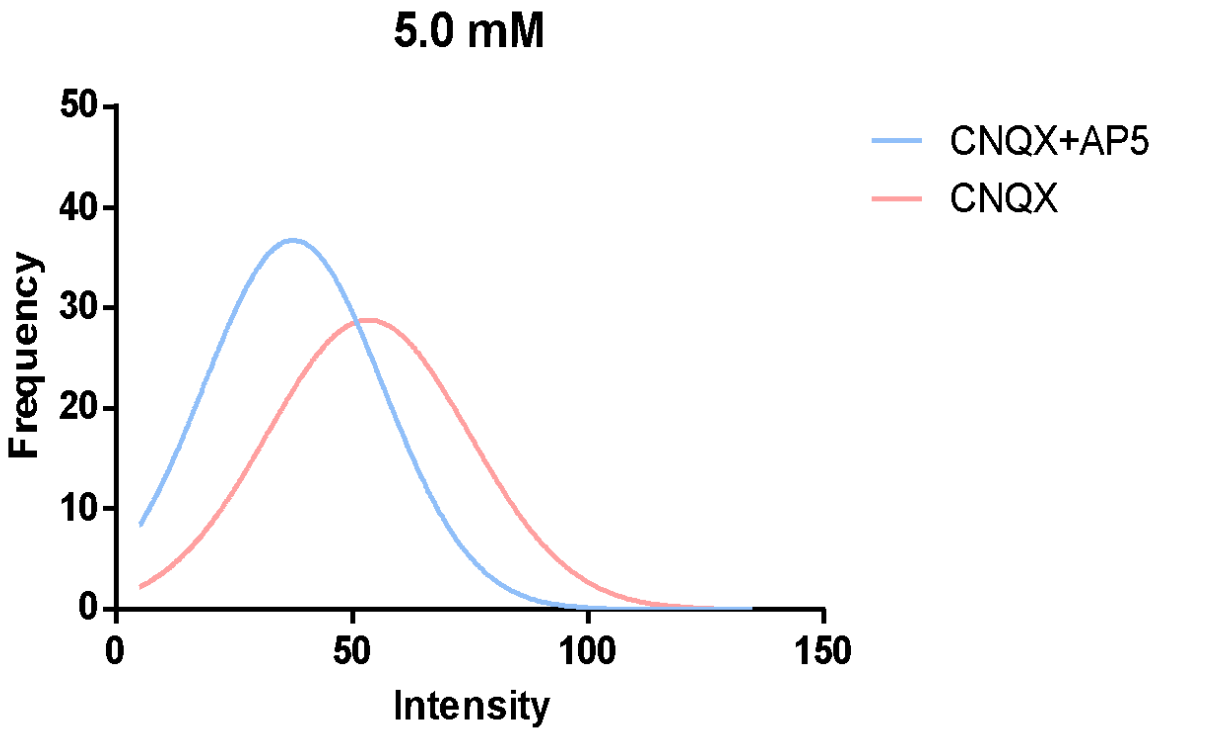
5.0 mM
Frequency
Intensity
0
10
20
30
40
50
0
50
100
150
CNQX+AP5
CNQX

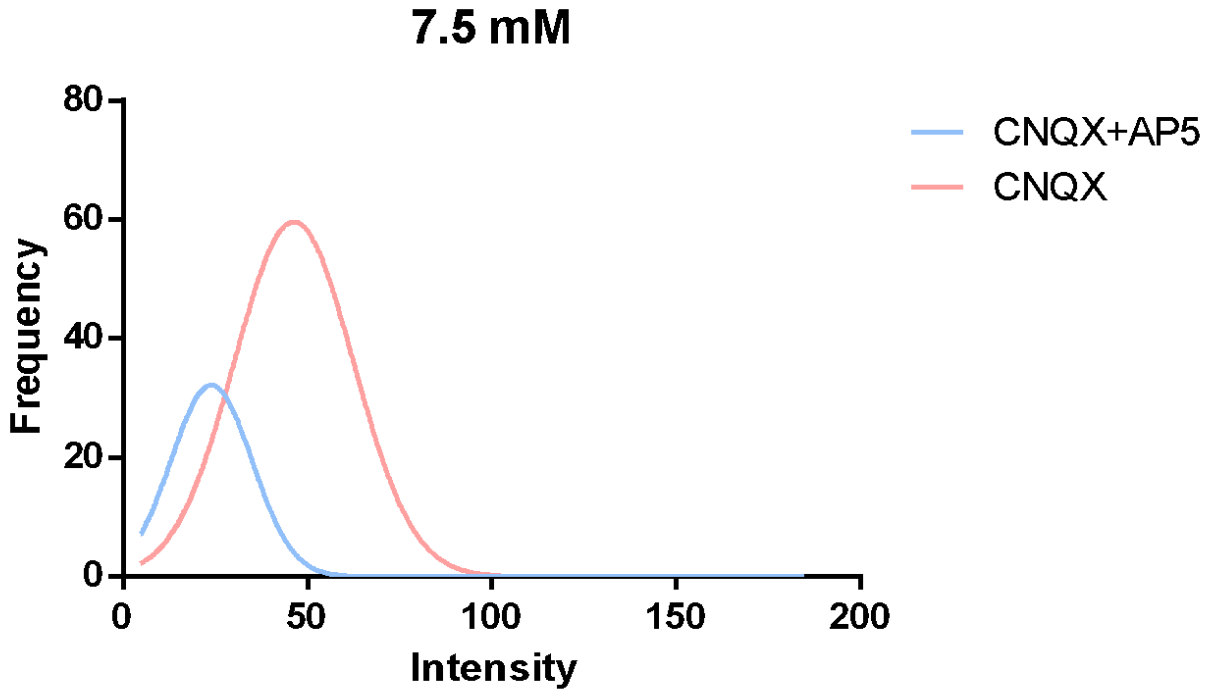
7.5 mM
Frequency
Intensity
0
20
40
60
80
0
50
100
150
200
CNQX+AP5
CNQX

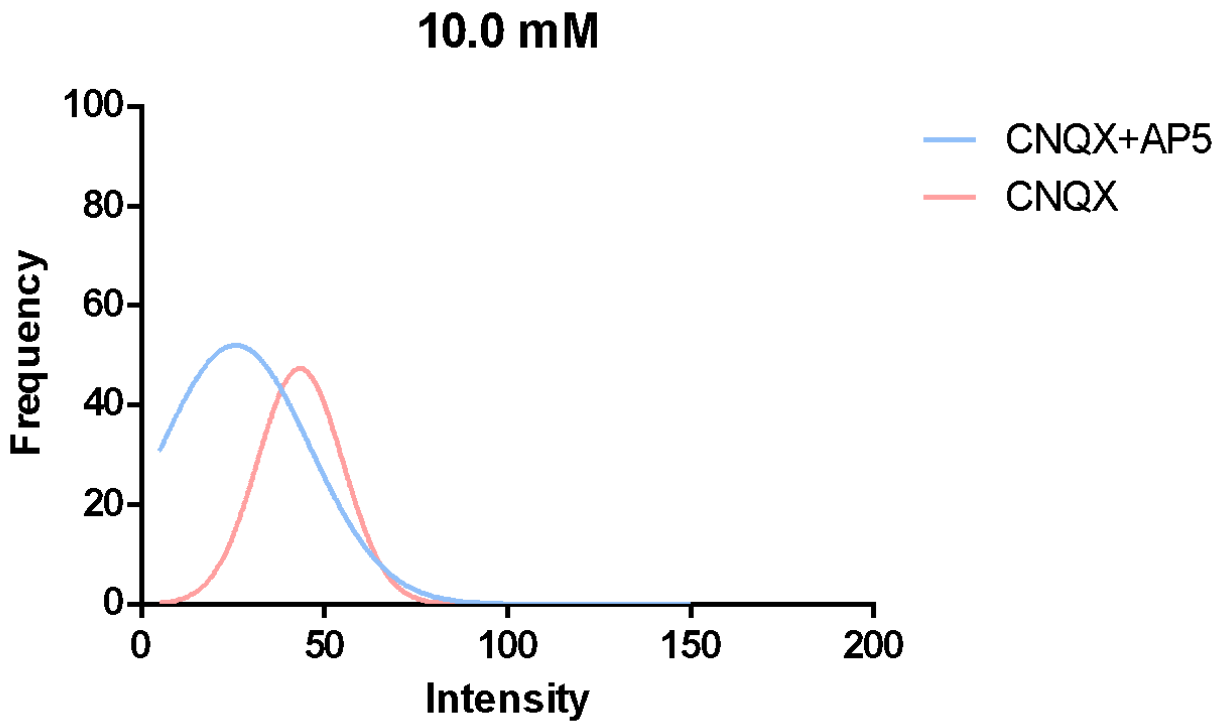

Figure 12: All figures depict a one to one comparison of the control (CNQX only) and experimental (CNQX+AP5) conditions for 6 different concentrations of Calcium -0.8, 1.0, 2.0, 5.0, 7.5, 10.0 mM.

Comparing CNQX versus CNQX+AP5 plots, the variance of the latter is greater than that of the former for all [Ca^{2+}]. This suggests a possible role of NMDARs in maintaining the heterogeneity of synaptic strengths, which collapses on blockage of these receptors through AP5 action.

4.7 Troubleshooting of FM 1-43 experiments on unsuccessful attempts at imaging:

Subsequent time was spent on troubleshooting for achieving 100 per cent success rate in FM 1-43 imaging. Following some attempts and change of rig (From Olympus BX51 to IX71 but there were no technical glitches associated with any of the rigs), the success rate reduced to 10 per cent that too with some degree of uncertainty. Following were the problems faced across different experiments–

A.) No loading of dye by 40APs at 20Hz. Imaging after washing showed no staining of boutons.

B.) Loading of dye but no unloading by (600APs at 20Hz) x 3 times. Imaging after

washing showed stained puncta but no destaining even after unloading stimulation.

C.) High background rise after unloading stimulation. These experiments were discarded due to inhomogeneous background across the timeline of experiment which rendered it technically difficult to subtract the measured intensities pre and post stimulation. This background rise contributes to fluorescence intensity of the puncta and hence, impair the experiment.

D.) Many cells were found to have swollen up and autofluorescent debris was found scattered on the cover slip, which contributed to the increase in background.

E.) Neurons in dissociated cultures are highly active and show a lot of spontaneous events (Huisheng Liu et. al., 2009). This sometimes leads to spontaneous firing and hence loading of boutons. Therefore, vesicle loading can be seen in experiments in which the stimulation electrode is dysfunctional leading to false positives.

Applied solutions for resolution of the issues and discussion

a.) Cell health was the first concern addressed since vigour of cells varies from batch to batch every week. Therefore, osmolarity and pH of Extracellular Buffer Solutions was looked at before and after making up with CNQX, Picrotoxin and FM1-43.

- pH turned out to be the same – 7.3.
- Osmolarity increased by around 17-20mOsm (from 310 to 330) after adding the drugs and dye. This was attributed to error in Osmometer reading since the expected rise in osmolarity was about 1-2mOsm.
- Even so, solutions with lower osmolarity (280 mOsm) were made to test out the health of cells on exposing to the drugs and dye containing EBS.
- Still, a number of cells were found to be unhealthy. On continuous analysis of cells under microscope from start of the experiment, it was found that some highly dense islands of cells were already unhealthy and reasons were attributed to excessive cell number per unit area, and resource competition.

b.) The **stimulation electrode** was tested for active stimulation before each experiment by dipping in EBS and running a voltage of 100 Volts at 200 Hz at monophasic mode. Bubbles corresponding to electrolysis were observed every time and it was concluded that the electrode is in working condition.

- Destaining trials by changing potential difference to 20V, 30V and 40V for monophasic stimulation were performed subsequently on the same neuron. For biphasic stimulation, potential was raised from 40 to 60 to 80 Volts. Unloading was not observed however, destaining was seen after 45mM K+ EBS perfusion. This led to further scrutiny of the electrode by doing Calcium imaging.
- Cells were labelled with Fluo-4 Acetomethyl (AM) ester Calcium dye and checked for Calcium responses under electrode stimulation.
- It was observed that the stimulation threshold varies from cover slip to cover slip ranging from 10 Volts to 70 Volts (Mono/Biphasic stimulation). Representative data of neuronal spiking is presented below. Conditions are specified with each data set.

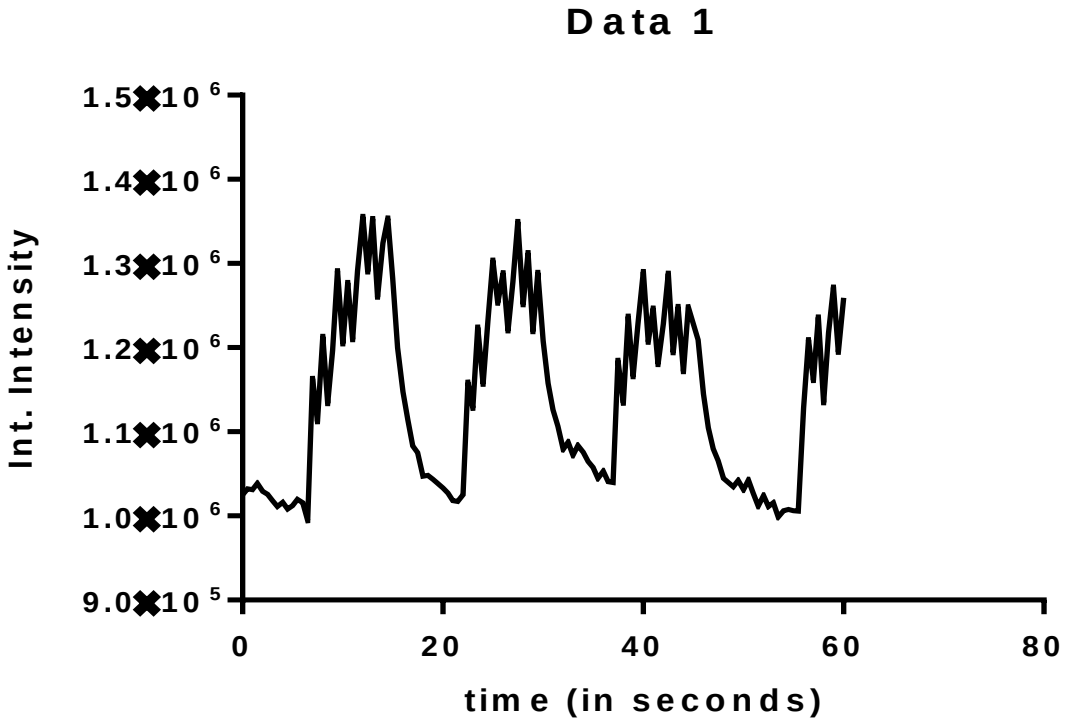

Figure 13.1 y axis – Integrated intensities of soma of a neuron calculated on metamorph. X axis – time in seconds of the time lapse.

Condition: Imaging period = 0.5 seconds. Stimulation every 7.5 seconds (15 planes). Monophasic pulse 1 Hz for 7 seconds, 40 Volts, gradually decreasing till 20 Volts.

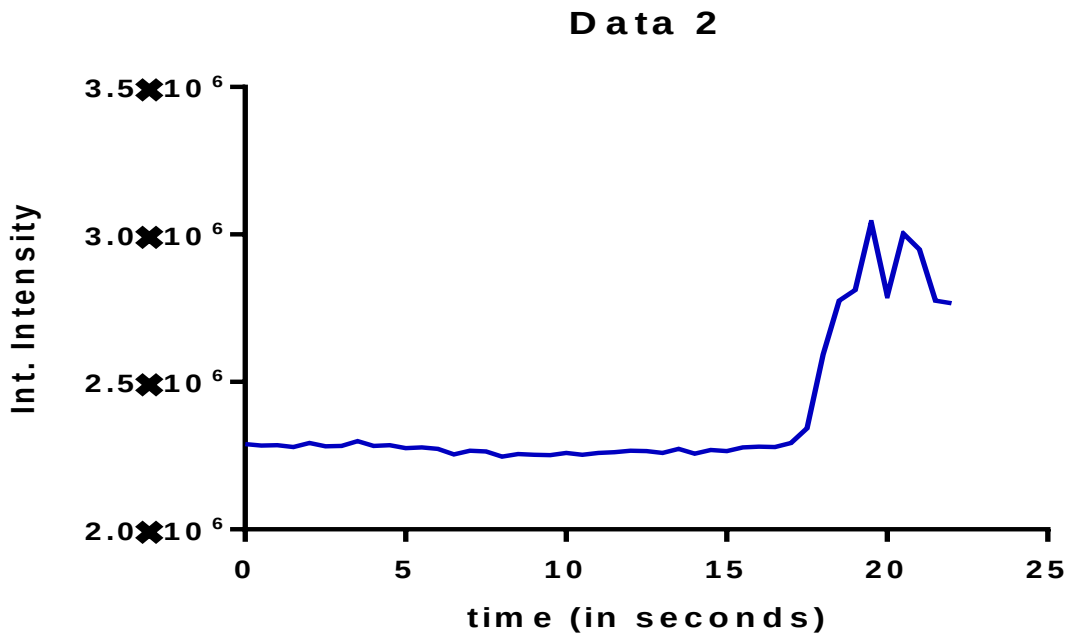

Figure 13.2 y axis – Integrated intensities of soma of a neuron calculated on metamorph. X axis – time in seconds. Voltage is gradually increased with time and neuron starts spiking at t = 37s.

Condition: Imaging period= 7.5 seconds. Stimulation frequency – 10 Hz. Gradual increase in voltage from 1 to 10 Volts in 22.5 seconds. Cell starts spiking at V = 9 Volts Biphasic pulse.

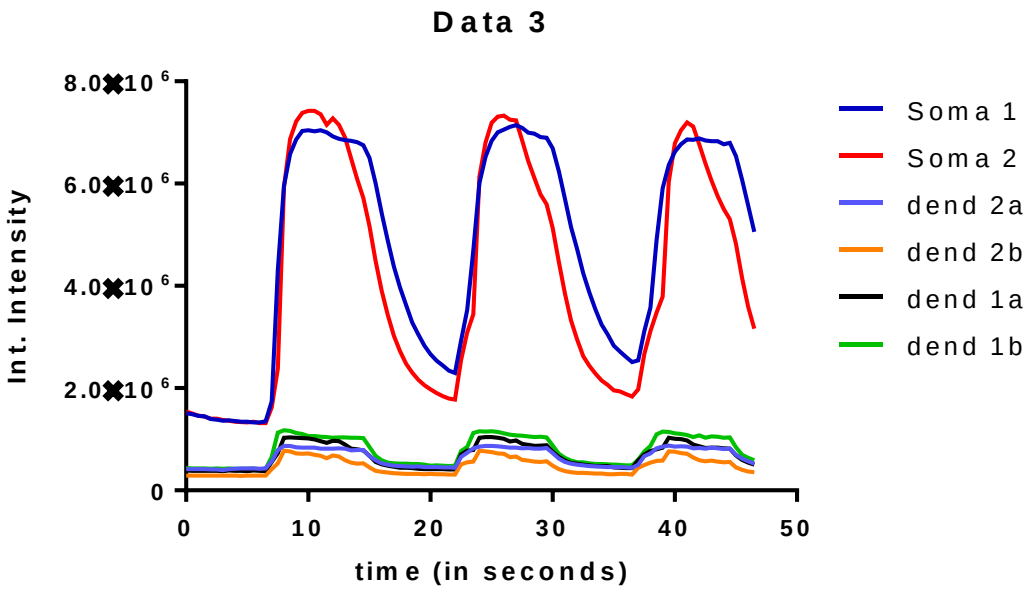

Figure 13.3 y axis – Integrated intensities of 2 neurons on metamorph. X axis – time in seconds. Soma1, dend1 correspond to the first neuron and soma2, dend2a,b to the soma and 2 dendrites of the second.

Condition: Frequency = 20Hz. Voltage – 80 Volts (Biphasic). Stimulation times – 10 seconds with interval time of 10 s.

- Threshold changed from neurons to neurons and the stimulation electrode was deemed as functional but the stochasticity associated with its reliability part shifted from the electrode to the neurons. Calcium imaging has a stronger optical signal and does not require visualizing synaptic puncta. After one or two trials, cells reliably respond to the stimulation. However, this visualization is difficult in punctate staining of FM 1-43 dye due to uncertainty in deciding whether the puncta are a result of a spontaneous or a stimulation-evoked release event (issue addressed in section c).

- Interpretations could be either the neurons required “waking up” from the silent state to a responsive state (by exposure to silencing drugs, neurons become silent and slight depolarization of membrane sometimes might be necessary to bring them into active state) or just that the threshold of field stimulation was different.

c.) To avoid loading by spontaneous firing, neurons were treated with CNQX and Picrotoxin for 10 minutes prior to incubation in FM 1-43 dye. It is expected that

the spontaneous firing stop and only spontaneous release events are left. Loading due to spontaneous release is weak and practically no signal is observed. On the other hand, direct exposure of the cover slip to FM 1-43 solution without prior incubation in drugs causes substantial labelling of synapses and it is difficult to make out difference between action potential dependent and spontaneous loading.

- In the former case, loading is essentially null and hence, there is no subsequent destaining. But the spontaneously labeled (due to spontaneous vesicle recyling vesicles destain on exposure to depolarization by 45mM KCl containing EBS (It is a standard paradigm for strongly stimulating neurons by providing high external K+ for sustenance of Action potential firing).

- In the latter case, destaining success rate was stochastic, with unloading visible in some cases and in others, not. But 45 mM KCl containing EBS caused neuron wide destaining of all synapses.

- These experiments further supported the fact that the stimulation electrode is ineffective in stimulating the neurons.

- Substitution of one electrode was done with a new electrode but the stochasticity remained.

4.8 Detection of astrocytic Calcium transients and the putative timing correlation with neuronal spiking:

As the troubleshooting of stimulation electrode progressed, a peculiar phenomenon specific to some neurons was observed.

A.) Astrocytic transients were seen to be propagating towards the dendrites of pyramidal neurons with their peak arising approximately 35-40 seconds after neuronal spikes (n = 4 neurons, 3 cover slips).

B.) During neuronal spiking, astrocytic Calcium signaling reduced significantly. However, transients through whole soma and processes surrounding dendrites were observed before and after stimulating neurons.

Since the stimulation electrode was reliably working for Calcium imaging and this observation tends to support the working model of the astrocyte dependent regulation of presynaptic strengths, it was important to note this aspect of Calcium dynamics. Representative data is presented below with experimental conditions.

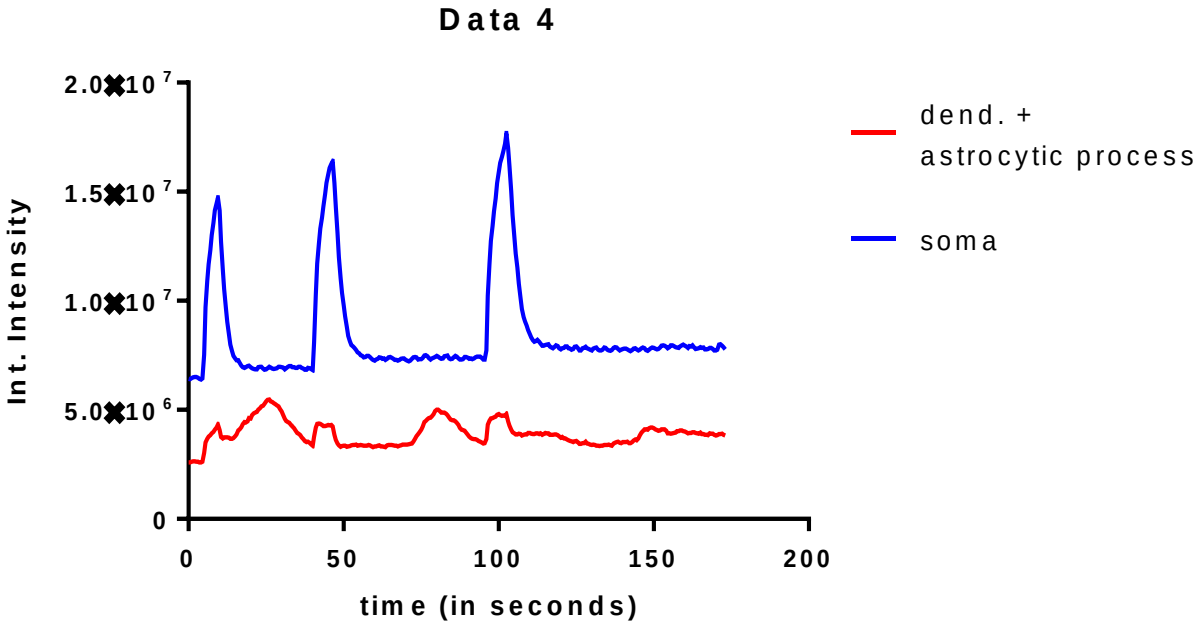

Figure 14.4 y axis – Integrated intensities one neuron and one astrocyte calculated on metamorph. X axis – time in seconds. Soma – soma of the neuron. Dend. + astrocytic process surrounding the dendrite both come under the ROI. Dendritic spikes with neuron but not astrocyte. Astrocyte transient occurs separately along the timecourse.

Condition: Biphasic stimulation – 3 trials: 20, 40, 80 Volts. Frequency: 20Hz. Stim. Period = 5 s. Interval 1 = 35 s. Interval 2 = 50 s.

In a typical experiment, neurons are stimulated and Calcium dynamics are monitored until astrocytic transients arise. Following this, neurons are stimulated again. As observed, the graph suggests rise in astrocyte Calcium levels surrounding the dendrite after a certain time lag. The red bumps appearing along with blue spikes are dendritic Calcium responses. The in-between ones are astrocyte responses on the dendrite.

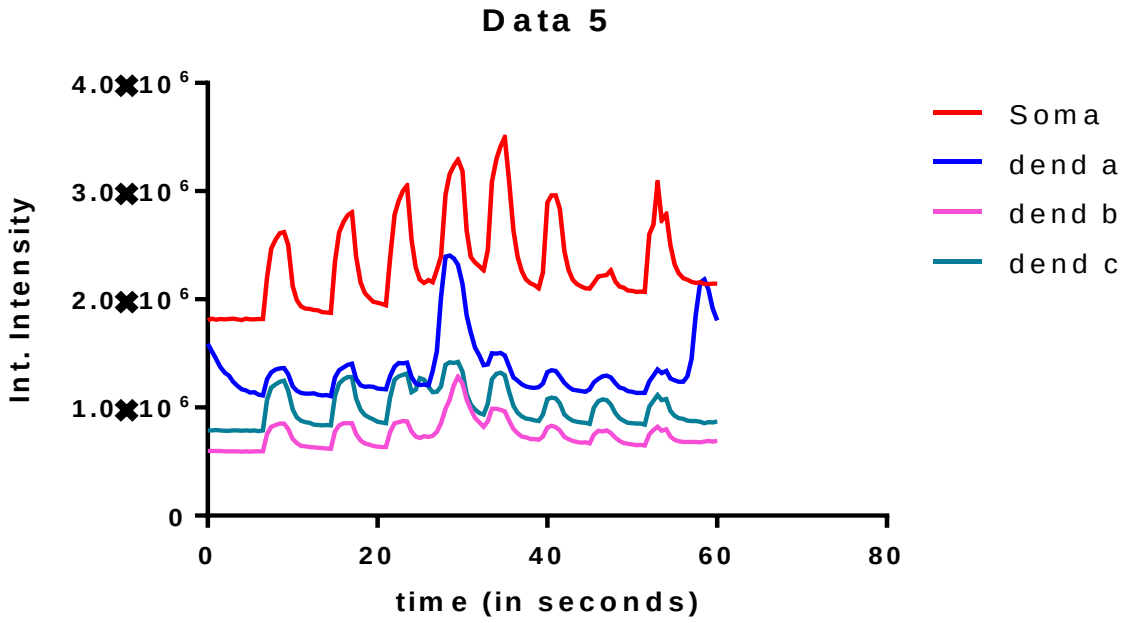

Figure 14.5 y axis – Integrated intensities of a neuron calculated on metamorph. X axis – time in seconds. Dend a,b,c are 3 dendrites of the neuron while astrocytic processes fall in their ROIs. Due to short stimulation interval, astrocytic transient tend to coincide with neuronal spikes. However, they still occur at a timescale of 30-40 seconds.

Conditions: Biphasic stimulation – 8 trials: Gradual increase from 40 to 90 Volts until trial 5. Gradual decrease onwards to 10 Volts followed by 60 Volts stimulation. Frequency: 20 Hz. Trial duration 5 seconds. Interval 5 seconds. Stim. Start – Plane 11.

This data set shows a rise in Calcium in Astrocytic processes surrounding different dendrites at around the same time (Plane 49 to 61 – t =24.5 s to 30.5 s) with a small shift in peaks by approximately 1 second.

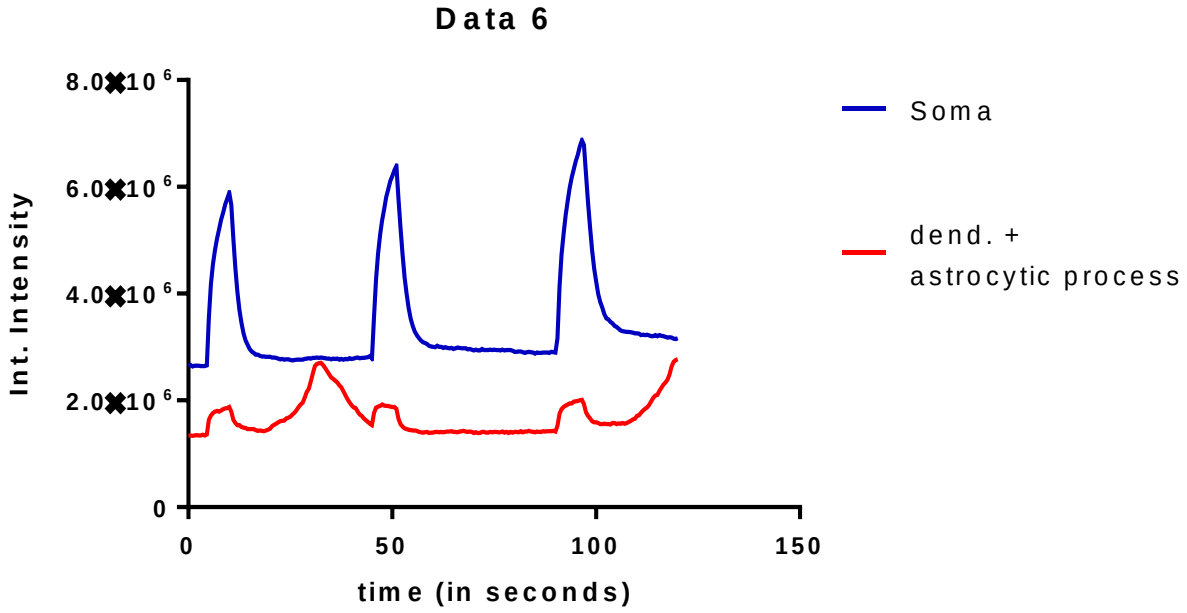

Figure 14.6 y axis – Integrated intensities of a neuron calculated on metamorph. X axis – time in seconds. Soma – soma of the neuron. Dendrite spiking can be seen coinciding with soma spike. The astrocytic process shows transients after 1st and 3rd neuronal spike and not 2nd.

Condition: Biphasic stimulation – 3 trials: 40, 50, 60 Volts. Frequency: 20Hz. Stim. Period = 5 s. Interval 1 = 35 s. Interval 2 = 40 s.

Here, signal from soma and dendrites are intact but signal from astrocyte process was silent after the second neuronal stimulation. It was, however, visible clearly after the first and third neuronal spike. To rule out the possibility of astrocytic activity occurring by spontaneously by chance, control experiment was done and no more than one spontaneous transients were seen at the same location of dendrite.

5. Discussion

To summarize, the results of this report supports the recent findings of a possible role of astrocytes in presynaptic strength regulation on a dendritic tree. First of all, consistent lowering of variance of strength distribution in the experimental condition of AP5 as compared to control provides evidence for homogenization (correlation) of strengths on astrocytic Calcium signaling blockade. The working model through which astrocytes are presumed to be regulating presynaptic strengths of inputs

neighboring to an excitatory synapse is depicted in figure 14.

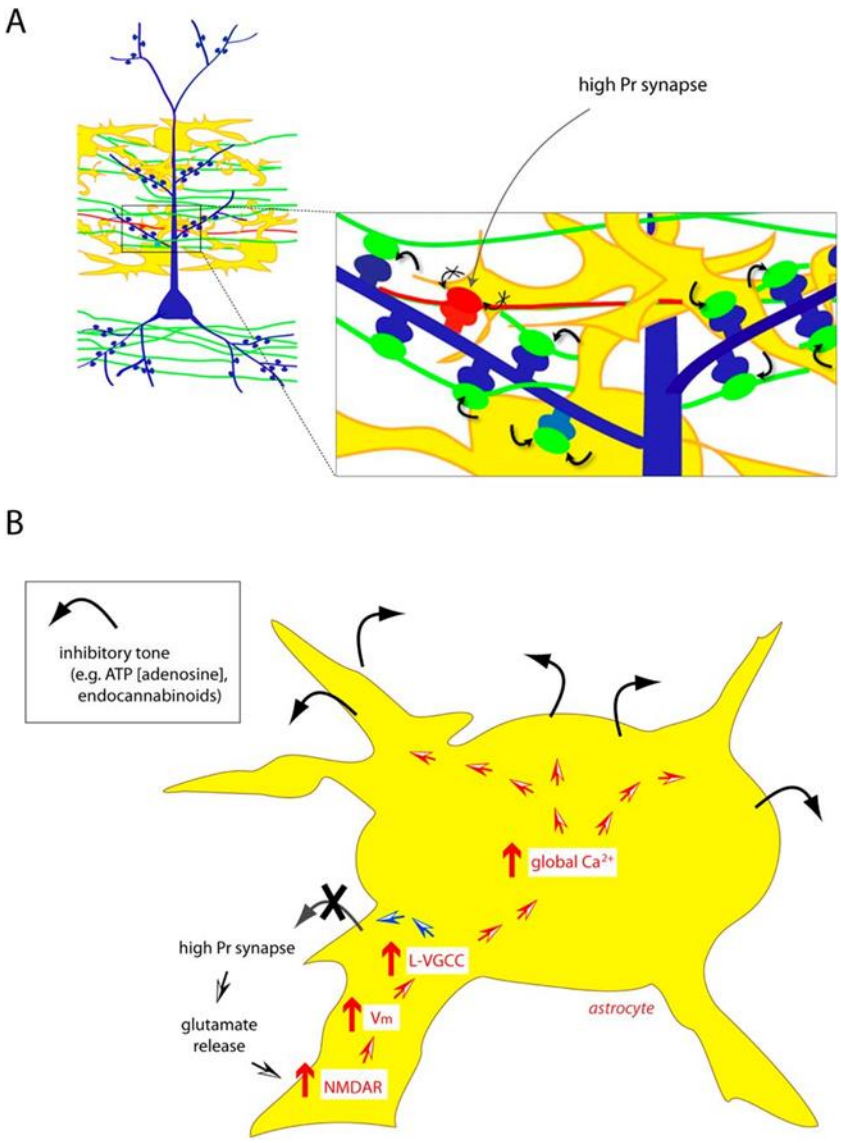

Figure 14. Working model for astrocyte-dependent decorrelation of presynaptic strengths. A) Illustration of tripartite synapses on a CA1 neuron and the inhibitory tone exerted by astrocytes. B) Glutamate released from high Pr synapses strengthens tonic inhibitory tone on excitatory synapses. (Figure taken from Letellier et.al. 2016)

An excitatory release event causes glutamate overflow in the synapse which is sensed by astrocytic NMDARs leading to Calcium influx. This depolarization event in the astrocytic process further opens up Voltage Gated Calcium Channels (VGCCs) and causes rise in the global Calcium levels. These global transients then travel to other processes wrapping neighboring synapses and render an inhibitory tone by releasing diffusible inhibitory gliotransmitters like endocannabinoids, ATP, adenosine

etc. Upon NMDAR blockade by AP5, a reduced variance in the intensity distribution (which is taken as a direct correlate of Pr) is noted which is presumably caused by hampering the inhibitory tone resulting from astrocytic Calcium signaling. Although the result seems somewhat convincing but the study has some caveats associated with it - first, comparison amongst old age of cells (DiV 20-24) is usually not the approach of tackling such problem as developmental effects can influence the expression of channels, receptors and even the rates of vesicle recycling. Still, experiments were carried out based on the presumption that this astrocyte-dependent regulation is common across dissociated cultures and acute slices, wherein the slice experiments were carried out in adult mice and the culture experiments in young cells (DIV 11-16) in the previous study (Letellier et.al., 2016). Second, the combination of drugs used in these experiments was varied from condition to condition, for instance, picrotoxin was used only in a subset of experiments. Although theoretically, there should not be any non-specific effect if only CNQX is used since it blocks recurrent firing and hence, stops excitatory as well as inhibitory transmission, consistency in experimental conditions is expected. The number of synapses were sufficient for analysis but the number of coverslips were less. A thorough analysis usually requires an N of 5-7 to establish a result. Additional experiments will be carried out during the remaining time to gather more N numbers. The second part of results demonstrated astrocyte calcium dynamics as a neuronal activity dependent phenomenon. One can speculate with some degree of certainty that Calcium transients in astrocyte processes surrounding dendrites implies at least uni-directional communication at the tripartite central synapses. Astrocyte calcium dynamics are implicated in a wide array of intra and extracellular signaling pathways (Araque et.al., 2014). On this train of argument, it can further be hypothesized that some form of homeostatic regulation could be taking place during the period following neuronal firing at synapses via astrocytes. Indeed, stricter analysis is required for concluding anything with certainty, but it provides a temporal window (35-40s after stimulation) to look at neuron-astrocyte interactions at the very least. A possible experiment could be to bath apply an ATP blocker and measure the variance of presynaptic strengths before and after the Calcium transients in

astrocytic processes wrapping the dendrites using FM 4-64 (excitation/emission – 520/640). The troubleshooting measures for technical problems associated with FM 1-43 experiments led to this peculiar observation of timing of astrocyte Calcium transients. Although the stimulation electrode is reliable enough to perform Fluo-4 AM Calcium imaging due to strong optical signal and longer time of stimulation and imaging, it still is difficult to go ahead with FM 1-43 labeling as a weaker signal and uncertainty of spontaneous or evoked release event stalls the conclusion of experimental success. Remaining options include replacement of platinum electrodes or switching to a completely different chamber, which will be tried and tested during the remainder of time. It is of extreme importance to understand the mechanisms responsible for maintaining stability of a neural network. The hebbian plasticity mechanisms are important for information storage but at the same time pose as a potential destabilizing threat for the network. This threat is thought to be counterbalanced by local as well as global homeostatic mechanisms. Emerging role of astrocytes as a key player of this stabilizing force motivates the study. Speaking further, malfunctioning of glutamate and K+ clearance is heavily implicated in epilepsy (Coulter & Eid, 2012). The expression of glutamate transporters (EAAT1/2) is abnormal and found to be reduced or redistributed in epilepsy models (Christian Steinhäuser and Gerald Seifert, 2012). Increase in extracellular glutamate concentration (from nM to µM) owing to this and dysfunctionality of glutamate synthase enzyme, which converts glutamate to glutamine results in excitotoxicity and neuronal death. Thus, this regulation plays a homeostatic role in placing a ceiling on the overall excitability of the postsynaptic neuron by adjusting Prs of the presynaptic inputs. Evidences also suggest activation of neuronal and glial NMDAR, and mGluR (Inyushin & Eaton, 2010), resulting in epileptic seizures. Another potential effect could be the impaired distribution of inhibitory or excitatory gliotransmitters at the destined synapses. For instance, high localisation of glutamate at glutamatergic synapses might result in seizure events. Thus, astrocytes can play a role in distribution, rather, dissipation of activity across the network through gap-junctions by releasing inhibitory transmitters at excitatory synapses and *vice versa*. Therefore, probing deeper into this regulatory mechanism will yield

potential therapeutic insights into treatment of neurodegenerative disorders.

6. Future directions:

6.1 Alternative live-labeling approach – Anti-synaptotagmin/AMPA receptors antibody labeling:

Synaptotagmin I is a Calcium sensing membrane trafficking protein which takes part in Calcium-evoked synaptic vesicle fusion. Its vesicular luminal domain component is exposed to the extracellular space during exocytosis (Dobrunz and Stevens, 1996; Dobrunz, 2002; Regehr et. al., 2009). The αsytI oyster conjugated 488 antibody (Green) binds to the luminal domain and fluoresces when endocytosed. To confirm an excitatory synapse, we plan to live-label the GluR2/3 subunits of AMPA receptor by GluR2/3 Oyster 550 antibody [Red] against the extracellular domain. Thus, these antibodies can also be used to monitor presynaptic strengths of excitatory neurons in ways similar to FM 1-43 dye.

6.2 VGLUT-pHluorin experiments for confirming NMDAR involvement.

VGLUT-pHlourin is a genetically encoded optical indicator for vesicle release and recycling. It is a fusion of vesicle glutamate transporter with super-ecliptic pHluorins on the luminal domain. Ecliptic pHluorins are typically Green Fluorescent protein (GFP) derivatives with a shift in pH sensitivity. Their fluorescence is quenched when vesicles are inside the acidic vesicle, ready to be released. Exposure of the protein to the basic nature of EBS on vesicular exocytosis relieves the quenching and subsequent reacidification on endocytosis quenches it again. This process can be exploited to monitor the synaptic strengths of a single neuron in a way similar to FM dye experiments. Experiments will be repeated in the presence and absence of AP5 and fluoroacetate (Rizo and Xu, 2015; Sudhof, 2004; He and Wu, 2007).

6.3 Treating cultures with Fluoroacetate.

Fluoroacetate disrupts astrocyte metabolism by disrupting the Kreb's cycle process and blocking ATP production (Regehr et.al., 2009). It preferentially disturbs astrocyte function and rules out chances of any energy dependent

Calcium release from its stores. Some preliminary data is obtained and further FM labeling and VGLUT pHluorin experiments will be carried out with Fluoroacetate.

6.4 Patching astrocyte and perfusing BAPTA with FM/VGLUT experiments.

1,2-bis[2-aminophenoxy]ethane-N,N,N',N'-tetraacetic acid (BAPTA) is a calcium buffer, which can be used to reduce free Ca2+ ions. As a result, an increase in correlation of strengths should be seen through FM-labelling and VGLUT-pHluorin.

6.5 Looking at pre and postsynaptic matching and the effect of astrocyte function knockdown on the same.

It is known that the release probability is correlated with GluR2 subunit population in postsynaptic AMPA receptors in an activity dependent manner (Branco and Staras, 2009). We plan to extend this analysis to the population of GluR2/3 subunits and attempt at monitoring this matching in on and off astrocytic Calcium.

6.6 Using DREADDs (Designer Receptors Exclusively Activated by Designer Drugs) for chemogenetically hyperpolarizing astrocytes paired with imaging of presynaptic strengths by FM 1-43 dye.

DREADDs are modified G-protein coupled receptors, which are sensitive to an exogenously applied ligand (e.g. CNO cyanate). Different types of DREADDs can be used to either de- or hyperpolarize cells. Thus, expressing a hyperpolarizing DREADD in astrocytes can be used as another means of investigating the effect of astrocytes on presynaptic strengths.

7. References:

A. Serrano, et al. GABAergic network activation of glial cells underlies hippocampal heterosynaptic depression. J. Neurosci., 26 (2006), pp. 5370–5382.

Activity-Dependent Regulation of Synapses by Retrograde Messengers. Wade G. Regehr,* Megan R. Carey, and Aaron R. Best. Neuron. 2009 Jul 30; 63(2): 154–170.

Activity-dependent coordination of presynaptic release probability and postsynaptic GluR2 abundance at single synapses. Hirofumi Tokuoka and Yukiko Goda Proc.Natl.Acad.Sci.U.S.A. 14656–14661, doi: 10.1073/pnas.0805705105.

Araque, et al. Tripartite synapses: glia, the unacknowledged partner. Trends Neurosci., 22 (1999), pp. 208–215.

Arnth-Jensen N, Jabaudon D, Scanziani M (2002) Cooperation between independent hippocampal synapses is controlled by glutamate uptake. Nat Neurosci 5:325–331, doi:10.1038/nn825, pmid:11896395.

Astrocyte calcium signaling: the third wave. Narges Bazargani & David Attwell. Nature Neuroscience 19, 182–189 (2016) doi:10.1038/nn.4201.

Astrocyte dysfunction in epilepsy. Christian Steinhäuser and Gerald Seifert. Jaspers basic mechanisms of Epilepsies.

Astrocytes regulate heterogeneity of presynaptic strengths in hippocampal networks. Mathieu Letellier, Yun Kyung Park, Thomas E. Chater, Peter H. Chipman, Sunita Ghimire Gautam, Tomoko Oshima-Takago, and Yukiko Goda. E2685–E2694, doi: 10.1073/pnas.1523717113.

Autapses and networks of hippocampal neurons exhibit distinct synaptic transmission phenotypes in the absence of synaptotagmin. Huisheng Liu, Camin Dean, Christopher P. Arthur, Min Dong, and Edwin R. Chapman. J Neurosci. 2009 Jun 10; 29(23): 7395–7403.doi: 10.1523/JNEUROSCI.1341-09.2009

Bacci, A. et al. Chronic blockade of glutamate receptors enhances presynaptic release and downregulates the interaction between synaptophysin-synaptobrevin-vesicle-associated membrane protein 2. J. Neurosci. 21, 6588–6596 (2001).

Bergles DE, Jahr CE (1997) Synaptic activation of glutamate transporters in hippocampal astrocytes. Neuron 19:1297–1308, doi:10.1016/S0896-6273(00)80420-1, pmid:9427252.

C. Allen, C.F. Stevens An evaluation of causes for unreliability of synaptic transmission Proc. Natl. Acad. Sci. USA, 91 (1994), pp. 10380–10383.

C. Rosenmund, J.D. Clements, G.L. Westbrook. Nonuniform probability of glutamate release at a hippocampal synapse. Science, 262 (1993), pp. 754–757.

C.F. Stevens, Y. Wang Facilitation and depression at single central synapses. Neuron, 14 (1995), pp. 795–802.

C.F. Stevens, Y. Wang. Changes in reliability of synaptic function as a mechanism for plasticity. Nature, 371 (1994), pp. 704–707.

Cajal SR 1894. La fine structure des centres nerveux. Proc R Soc Lond 55: 444–468

Danbolt NC (2001) Glutamate uptake. Prog Neurobiol 65:1–105, doi:10.1016/S0301-0082(00)00067-8, pmid:11369436.

Definition of the Readily Releasable Pool of Vesicles at Hippocampal Synapses. Christian Rosenmund, Charles F Stevens. Neuron. Volume 16, Issue 6, June 1996, Pages 1197–1207.

Dendritic diameters affect the spatial variability of intracellular calcium dynamics in computer models Haroon Anwar, Christopher J. Roome3, Hermina Nedelescu, Weiliang Chen2, Bernd Kuhn3 and Erik De Schutter Front. Cell. Neurosci., 23 July 2014 | https://doi.org/10.3389/fncel.2014.00168

Dentritic spines: structure, dynamics and regulation. Heike Hering & Morgan Sheng. Nat Rev Neurosci. 2001 Dec;2(12):880-8.

Diamond JS (2005) Deriving the glutamate clearance time course from transporter currents in CA1 hippocampal astrocytes: transmitter uptake gets faster during development. J Neurosci 25:2906–2916, doi:10.1523/JNEUROSCI.5125-04.2005, pmid:15772350.

Diamond JS, Jahr CE (2000) Synaptically released glutamate does not overwhelm transporters on hippocampal astrocytes during high-frequency stimulation. J Neurophysiol 83:2835–2843, pmid:10805681.

Douglas JK, Wilkens L, Pantazelou E, Moss F (1993) Noise Enhancement of Information Transfer in Crayfish Mechanoreceptors by Stochastic Resonance. Nature 365: 337+.

Efficient coding in heterogeneous neuronal populations Mircea I. Chelaru and Valentin Dragoi.

PNAS (2008) 16344–16349, doi: 10.1073/pnas.0807744105.

Energy-Efficient Information Transfer by Visual Pathway. Synapses Julia J. Harris, Renaud

Jolive,Elisabeth Eng,David Attwell. Current Biology

DOI:http://dx.doi.org/10.1016/j.cub.2015.10.063. Volume 25, Issue 24, p3151–3160, 21

December 2015

Foster, M.; Sherrington, C.S. (1897). *Textbook of Physiology, volume 3* (7th ed.). London: Macmillan. p. 929.

Functional impact of dendritic branch point morphology. Michele Ferrante, Michele Migliore and Giorgio A. Ascoli. Journal of Neuroscience 30 January 2013, 33 (5) 2156-2165; DOI: https://doi.org/10.1523/JNEUROSCI.3495-12.2013

Futamachi KJ, Pedley TA (1976) Glial cells and extracellular potassium: their relationship in mammalian cortex. Brain Res 109:311–322.

Galante, M., Avossa, D., Rosato-Siri, M. & Ballerini, L. Homeostatic plasticity induced by chronic block of AMPA/kainate receptors modulates the generation of rhythmic bursting in rat spinal cord organotypic cultures. Eur. J. Neurosci. 14, 903–917.

Galli T, Haucke V. 2001. Cycling of synaptic vesicles: How far? How fast! Sci. STKE 88:RE1

Gandhi SP, Stevens CF. 2003. Three modes of synaptic vesicular recycling revealed by single-vesicle imaging. Nature 423:607–13

Glia. 2013 Feb;61(2):178-91. doi: 10.1002/glia.22425. Epub 2012 Oct 8. Heterosynaptic long-term depression mediated by ATP released from astrocytes. Chen J1, Tan Z, Zeng L, Zhang X,

Goda Y, Südhof TC. 1997. Calcium regulation of neurotransmitter release: reliably unreliable. Curr. Opin. Cell Biol. 9:513–18.

He Y, Gao W, Wu X, Li Y, Bu B, Wang W, Duan S.

Gliotransmitters travel in time and space. Araque A, Carmignoto G, Haydon PG, Oliet SH, Robitaille R, Volterra A. Neuron. 2014 Feb 19;81(4):728-39. doi: 10.1016/j.neuron.2014.02.007.

Hallermann S, Fejtova A, Schmidt H, Weyhersmüller A, Silver RA, Gundelfinger ED, Eilers J. Bassoon speeds vesicle reloading at a central excitatory synapse. Neuron. 2010;68:710–723.

He, L. & Wu, L. G. The debate on the kiss-and-run fusion at synapses. Trends Neurosci. 30, 447–455 (2007).

Heterogeneity of Release Probability, Facilitation, and Depletion at Central Synapses. Lynn E. Dobrunz, Charles F. Stevens. Neuron. Volume 16, Issue 6, June 1996, Pages 1197–1207.

J. del Castillo, B. Katz Quantal components of the end-plate potential. J. Physiol, 124 (1954), pp. 560–573

J.M. Zhang, et al. ATP released by astrocytes mediates glutamatergic activity-dependent heterosynaptic suppression. Neuron, 40 (2003), pp. 971–982.

Katz B. 1969. The Release of Neural Transmitter Substances. Liverpool: Liverpool Univ. Press

K.E. Sorra, K.M. Harris Occurrence and three-dimensional structure of multiple synapses between individual radiatum axons and their target pyramidal cells in hippocampal area CA1 J. Neurosci, 13 (1993), pp. 3736–3748

Local dendritic activity sets release probability at hippocampal synapses. Branco T1, Staras K, Darcy KJ, Goda Y. Neuron. 2008 Aug 14;59(3):475-85. doi: 10.1016/j.neuron.2008.07.006.

M. Raastad, J.F. Storm, P. Anderson. Putative single quantum and single fibre excitatory postsynaptic currents show similar amplitude range and variability in rat hippocampal slices. Eur. J. Neurosci, 4 (1992), pp. 113–117

Marvin JS, Borghuis BG, Tian L, Cichon J, Harnett MT, Akerboom J, Gordus A, Renninger SL, Chen TW, Bargmann CI, Orger MB, Schreiter ER, Demb JB, Gan WB, Hires SA, Looger LL (2013) An optimized fluorescent probe for visualizing glutamate neurotransmission. Nat Methods 10:162–170, doi:10.1038/nmeth.2333, pmid:23314171.

Miller RF, Dacheux R, Proenza L (1977) Müller cell depolarization evoked by antidromic optic nerve stimulation. Brain Res 121:162–166.

Moss F (2004) Stochastic resonance and sensory information processing: a tutorial and review of application. Clinical Neurophysiology 115: 267–281.

Mukherjee K, Yang X, Gerber SH, Kwon HB, Ho A, Castillo PE, Liu X, Südhof TC. Piccolo and bassoon maintain synaptic vesicle clustering without directly participating in vesicle exocytosis.

Proc Natl Acad Sci USA. 2010;107:6504–6509.

Murthy, V. N., Schikorski, T., Stevens, C. F. & Zhu, Y. Inactivity produces increases in neurotransmitter release and synapse size. Neuron 32, 673–682 (2001).

N.A. Hessler, A.M. Shirke, R. Malinow. The probability of transmitter release at a mammalian central synapse. Nature, 366 (1993), pp. 569–572

O. Pascual, et al. Astrocytic purinergic signaling coordinates synaptic networks. Science, 310 (2005), pp. 113–116 .

Optical detection of a quantal presynaptic membrane turnover. Timothy A. Ryan, Harald Reuter and Stephen J Smith. Nature 388, 478-482 (31 July 1997); Received 26 February 1997; Accepted 13 May 1997.

Orkand RK, Nicholls JG, Kuffler SW. Effect of nerve impulses on the membrane potential of glial cells in the central nervous system of Amphibia. J Neurophysiol. 1966;29:788–806.

Potassium Channel Activity and Glutamate Uptake are Impaired in Astrocytes of Seizure Susceptible DBA/2 Mice. Mikhail Inyushin, Lilia Y. Kucheryavykh, Yuriy V. Kucheryavykh, Colin G. Nichols, Russell J. Buono, Thomas N. Ferraro, Serguei N. Skatchkov, and Misty J. Eaton. Epilepsia. 2010 Sep; 51(9): 1707–1713. doi: 10.1111/j.1528-1167.2010.02592.x

Presynaptic Calcium Influx Controls Neurotransmitter Release in Part by Regulating the Effective Size of the Readily-Releasable Pool. Monica S. Thanawala and Wade G. Regehr. J Neurosci. 2013 Mar 13; 33(11): 4625–4633. doi: 10.1523/JNEUROSCI.4031-12.2013.

Purves D, Augustine GJ, Fitzpatrick D, et al., editors. Neuroscience. 2nd edition. Sunderland (MA): Sinauer Associates; 2001. Voltage-Gated Ion Channels. http://www.ncbi.nlm.nih.gov/books/NBK10883/

R. Malinow, N. Otmakhov, K.I. Blum, J.E. Lisman. Visualizing hippocampal synaptic function by optical detection of Ca2+ entry through the N-methyl-D-aspartate channel. Proc. Natl. Acad. Sci. USA, 91 (1994), pp. 8170–8174.

Release probability is regulated by the size of the readily releasable vesicle pool at excitatory synapses in hippocampus. Lynn E. Dobrunz. International Journal of Developmental Neuroscience

Reliable Neuronal Systems: The Importance of Heterogeneity. Johannes Lengler, Florian Jug, Angelika Steger. http://dx.doi.org/10.1371/journal.pone.0080694

Roitbak AI, Fanardjian VV (1981) Depolarization of cortical glial cells in response to electrical stimulation of the cortical surface. Neuroscience 6:2529–2537.

Rosahl TW, Spillane D, Missler M, Herz J, Selig DK, Wolff JR, Hammer RE, Malenka RC, Südhof TC. Essential functions of synapsins I and II in synaptic vesicle regulation. Nature. 1995;375:488–493.

Siksou L, Varoqueaux F, Pascual O, Triller A, Brose N, Marty S. A common molecular basis for membrane docking and functional priming of synaptic vesicles. Eur J Neurosci. 2009;30:49–56.

Spontaneous and evoked glutamate release activate two populations of NMDA receptors with limited overlap. Deniz Atasoy, Mert Ertunc, Krista L. Moulder, Justin Blackwell, ChiHye Chung, Jianzhong Su, and Ege T. Kavalali. J Neurosci. 2008 Oct 1; 28(40): 10151–10166. doi: 10.1523/JNEUROSCI.2432-08.2008.

Stein RB, Gossen ER, Jones KE (2005) Neuronal variability: noise or part of the signal? Nature Reviews Neuroscience 6: 389–397.

Stigloher C, Zhan H, Zhen M, Richmond J, Bessereau JL. The presynaptic dense projection of the Caenorhabditis elegans cholinergic neuromuscular junction localizes synaptic vesicles at the active zone through SYD-2/liprin and UNC-10/RIM-dependent interactions. J Neurosci. 2011;31:4388–4396

Sudhof, T. C. The synaptic vesicle cycle. Annu. Rev. Neurosci. 27, 509–547 (2004).

T. Schikorski, C.F. Stevens Quantitative ultrastructural analysis of hippocampal excitatory synapses. J. Neurosci., in press (1997)

The Presynaptic Active Zone. Thomas C. Südhof. Neuron. 2012 Jul 12;75(1):11-25. doi: 10.1016/j.neuron.2012.06.012.

The Synaptic Vesicle Release Machinery. Rizo J1, Xu J. Annu Rev Biophys. 2015;44:339-67. doi: 10.1146/annurev-biophys-060414-034057.

The computational power of astrocyte mediated synaptic plasticity. Rogier Min,* Mirko Santello, and Thomas Nevian. Front Comput Neurosci. 2012; 6: 93. Published online 2012 Nov 1. doi:10.3389/fncom.2012.00093, PMCID: PMC3485583

The probability of neurotransmitter release: variability and feedback control at single synapses. Tiago Branco1 & Kevin Staras. Nature Reviews Neuroscience 10, 373-383 (May 2009) doi:10.1038/nrn2634

Thiagarajan, T. C., Lindskog, M. & Tsien, R. W. Adaptation to synaptic inactivity in hippocampal neurons. Neuron 47, 725–737 (2005).

Thiagarajan, T. C., Piedras-Renteria, E. S. & Tsien, R. W. alpha- and betaCaMKII. Inverse regulation by neuronal activity and opposing effects on synaptic strength. Neuron 36, 1103–1114 (2002).

Tripartite synapses: astrocytes process and control synaptic information. Gertrudis Perea, Marta Navarrete, Alfonso Araque. Trends in Neurosciences. Volume 32, Issue 8, August 2009, Pages 421–431.

Urban N, Tripathy S (2012) Neuroscience: Circuits drive cell diversity. Nature 488: 289–290.

V.N. Murthy, T.J. Sejnowski, C.F. Stevens. Heterogeneous release properties of visualized individual hippocampal synapses. Neuron, 18 (1997), pp. 559–612.

Visualizing recycling synaptic vesicles in hippocampal neurons by FM 1-43 photoconversion Nobutoshi Harata, Timothy A. Ryan, Stephen J Smith, JoAnn Buchanan, and Richard W. Tsien. 2748–12753, doi: 10.1073/pnas.171442798.

Volume 20, Issues 3–5, June–August 2002, Pages 225–236.

Wierenga, C. J., Walsh, M. F. & Turrigiano, G. G. Temporal regulation of the expression locus of homeostatic plasticity. J. Neurophysiol. 96, 2127–2133 (2006).

Wiesenfeld K, Moss F (1995) Stochastic resonance and the benefits of noise: from ice ages to crayfish and SQUIDs. Nature 373: 33–36.

Zucker, R. S. & Regehr, W. G. Short-term synaptic plasticity. Annu. Rev. Physiol. 64, 355–405 (2002).